MICROENCAPSULATION OF HEALING AGENT FOR USE IN POLYMER COATINGS

A Major Project Report submitted in partial fulfillment for the award of the degree
Of

MASTER OF TECHNOLOGY

IN

POLYMER TECHNOLOGY

Submitted by
RAMAN DWIVEDI
(2K12/PTE/15)

Under the able guidance
of
Dr.P.K.ROY
SCIENTIST 'E'
CENTRE FOR FIRE, EXPLOSIVE AND ENVIRONMENT SAFETY (CFEES)
DEFENCE RESEARCH AND DEVELOPMENT ORGANIZATION (DRDO),
TIMARPUR DELHI-110054

&

Prof.D.KUMAR
HEAD OF DEPARTMENT
DEPARTMENT OF APPLIED CHEMISTRY AND POLYMER TECHNOLOGY
DELHI TECHNOLOGICAL UNIVERSITY (D.T.U)
(*Formerly Delhi College of Engineering*)
DELHI-10042

CERTIFICATE

This is to certify that this is a bonafide record of the M.Tech major project entitled **"MICROENCAPSULATION OF HEALING AGENT FOR USE IN POLYMER COATINGS"** has been submitted by Raman Dwivedi, for the award of the degree of "Master of Technology" in Polymer Technology is a record of bonafide work carried out by him. Raman has worked under our guidance and supervision and has fulfilled the requirements for the submission of the thesis. The project work has been carried out during the session 2013-2014.

To the best of our knowledge and belief the content therein is his own original work and has not been submitted to any other university or institute for the award of any degree or diploma.

Dr. D. KUMAR
Professor and Head of Department
Department of Applied Chemistry and Polymer Technology
Delhi Technological University (DTU),
Bawana Road, Delhi - 110042

Dr. P.K.ROY
Scientist 'E'
Centre for Fire, Explosive and Environment Safety (CFEES)
Defence Research and Development Organization (DRDO)
Timarpur, Delhi 110054

ACKNOWLEDGEMENT

I express my sincere thanks and deep sense of gratitude to my supervisors Dr. P.K.Roy (Scientist 'E',Centre for Fire, Explosive and Environment Safety (CFEES), DRDO) for his inspiring guidance, constant encouragement and motivation throughout the course of this work. To him I owe more than words can say and Prof.D.Kumar (D.T.U) for guiding me and helping me in all ways throughout my course work.

I take this opportunity to thank Dr. Chitra Rajagopal, Director, CFEES for giving me this opportunity to carry out this project work in their esteemed laboratory. I would also like to thank group members of EnSG like Ms Surekha Parthsarathy, Mr. Rajesh Chopra, Mr. Naveen Saxena, Mr. Saurabh Chaudhary, and Ms Manju for their immense support and guidance that helped me in completing the project.

I thank all the members of Centre for Fire Explosive and Environment Safety (CFEES) for their kind cooperation.

I thankfully acknowledge my family members and friends whose inspiration and motivation brought me to the completion of this project. This was a great learning experience and I will cherish it throughout my life.

Dated (Raman Dwivedi)

LIST OF FIGURES

LIST OF SCHEMES

Abstract

Different healing agents, namely unsaturated polyester and epoxy were encapsulated in polystyrene by physical encapsulation technique. The effect of operating parameters on the microcapsule dimensions and morphology was established by SEM imaging. Thermal and structural properties of the microcapsules were determined by TGA and FTIR respectively. Core content of PS encapsulated microcapsules was found to be 45 ± 3%. Epoxy and USP were encapsulated in urea-formaldehyde microcapsules by emulsion polymerisation process. The core content of the microcapsules was determined by solvent extraction method and was found to be 58± 4%. Latent hardener (copper complex of 2-methyl imidazole) was synthesized by the reaction of copper chloride with 2 methyl imidazole. Self-healing composites are also prepared by dispersing varying amount of microcapsules (10-30% w/w) in the matrix. The impact strength was found to decrease with introduction of microcapsules in the composition. Latent hardener was used as a curing agent to effect self healing in epoxy compositions containing epoxy encapsulated in UF microcapsules. Self healing efficiency was determined as the ratio of impact strength of the samples before and after healing. ~67% efficiency could be achieved using copper complex as the latent hardener system. Self healing was also demonstrated in compositions containing unsaturated polyester encapsulated in UF microcapsules. Although USP underwent thermal self curing, the temperature required could be brought down significantly by using AIBN as the free radical initiator. Self healing efficiency of ~103% could be achieved using AIBN as the curing agent.

CHAPTER 1: INTRODUCTION AND LITERATURE SURVEY

Introduction

The modern world uses a large variety of synthetic polymers in daily life and industry. The current society can be said to be living in "polymer age" due to the use of many synthetic polymer materials. However, there is a significant difference between natural biomaterials and artificial polymers. Natural biomaterials such as our human body can automatically heal damage or injury, while conventional synthetic polymers do not have this self-healing property.

To replace traditional materials various types of polymers with high functionality and advanced properties are being developed. These polymers sometimes are used in severe environments, such as the deep ocean or space, which are difficult to access. In addition, some polymers are used inside the human body, such as artificial organs and bone cement. Degradation, damage and failure are natural consequences of these material applications. Engineering research has been focused traditionally on either the design of new materials with increased robustness or the development of non-destructive evaluation methods for material inspection, yet all engineered materials eventually fail. The detection of damage and repair to these advanced materials is difficult even though their failure results in considerable expense and loss of effort and time. Thus, the importance of a healing effect in synthetic polymers is much more necessary for advanced applications. In contrast, biological systems approach this same dilemma in an elegant fashion by self-healing.

1.1 Self-healing materials

Self-healing materials exhibit the ability to repair themselves and to recover functionality using the resources inherently available to them. Whether the process is autonomic or externally assisted (e.g., by heating), the recovery process is triggered by damage to the material. Self-healing materials offer a new route toward safer, longer-lasting products and components[1]. There are variety of self-healing systems which have been developed for protective coatings, electronic

self-healing and mechanical self-healing. Out of these, compartmentalized self-healing systems require encapsulation of healing agents which in turn are incorporated into a polymer matrix. Due to its simplicity, low cost and the relatively high volume of healing agent delivered, much work has been done towards implementing the system in a variety of applications using a variety of chemistries.

1.2 Approaches to Self-Healing

Self-healing polymers and polymer composites can be classified into two categories:

(i) Intrinsic: that are able toheal cracks by the polymers themselves, and

(ii) Extrinsic: in which the healing agent has to be preembedded in the matrix. Extrinsic self healing approach involves inclusion of capsules or a 3D network containing the healing agent and these are usually classified as follows:

a) Capsule Based Healing
b) Vascular Healing

1.2.1. Intrinsic self-healing

Intrinsic self-healing polymers utilize the inherent ability of the material to self-heal, triggered either by a damage or in combination with an external stimulus.Thus, the so-called intrinsic self-healing polymers are based on specific property of the polymers thatenables crack healing under certain stimulation(mostly heating). The predominant molecular mechanisms responsible for the healing processes are based either on physical interactions or chemical interactions. These materials possess a latent functionality that triggers self-healing of damage via thermally reversible reactions, hydrogen bonding, ionomeric arrangements, or molecular diffusion and entanglement.

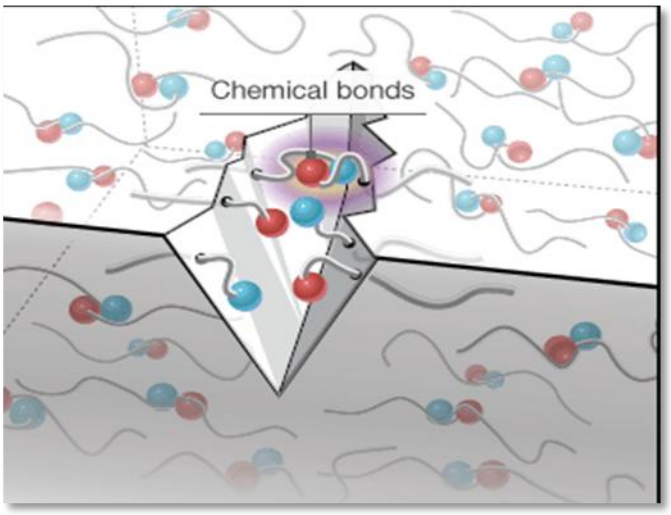

Figure1.1: Schematic of intrinsic self-healing

It is to be noted that although the intrinsic healing approaches are elegant but these are limited to small damage volumes because intimate material contact is required to ensure healing.

- **Self-healing based on physical interactions**

Compared to thermosetting polymers,crack healing in thermoplastic polymers had received more attention earlier. The healing process goes through five phases: (i) surface rearrangement,which affects initial diffusion function andtopological feature; (ii) surface approach, related tohealing patterns; (iii) wetting, (iv) diffusion, the main factor that controls recovery of mechanical properties, and (v) randomization, ensuring disappearance of cracking interface.

- **Self-healing based on chemical interactions**

Cracks and strength decay might be a result of structural changes in the polymers, like chain scission. One of the repairing strategies is inverse reaction,.i.e.recombination of the broken molecules. Such method does not focus on cracks healing but on ‘nanoscopic’deterioration. One example is polycarbonate (PC) synthesized by ester exchange method.

1.2.2. Extrinsic self-healing

In the case of extrinsic self-healing, the matrix resin itself is not inherently healable. In other words, extrinsic self-healing concept requires that the healing agents are pre-embedded into a

(polymeric) matrix enabling their release during a rupture event. As soon as the cracks destroy the fragile capsules, the healing agent is released into the crack plane due to capillary effect, which undergo polymerisation, resulting in healing of the crack. In accordance with types of containers, there are two modes of the repair activity: (i) self-healing in materials containing healant loaded pipelines, and (ii) self-healing in materials containing healant loaded microcapsules. Taking the advantages of crack triggered delivery of healing agent, manual intervention (e.g. heating required for intrinsic self-healing) might be no longer necessary.

1.3 Hollow glass tubes and glass fibers

The core issue of this technique lies in filling the brittle-walled vessels with polymerizable medium, which should remain in the fluid state at least at the healing temperature. Subsequent polymerization of the monomers flowing into the damage area leads to crack elimination. Dry [2] first identified the potential applicability of hollow glass tubes towards self healing. Accordingly, three types of healing system were developed (Figure 1.2)

(i) Single-part adhesive: All hollow pipettes contained only one kind of resin like epoxy particles (that can flow upon heating and get cured by residual hardener) or cyanoacrylate (that can be consolidated under the induction of air).

(ii) Two-part adhesive. In general, epoxy and its curing agent were used in this case. They were filled into neighboring hollow tubes, respectively.

(iii)Two-part adhesive. One component was incorporated into hollow tubes and the other in microcapsules [3].

(iv)

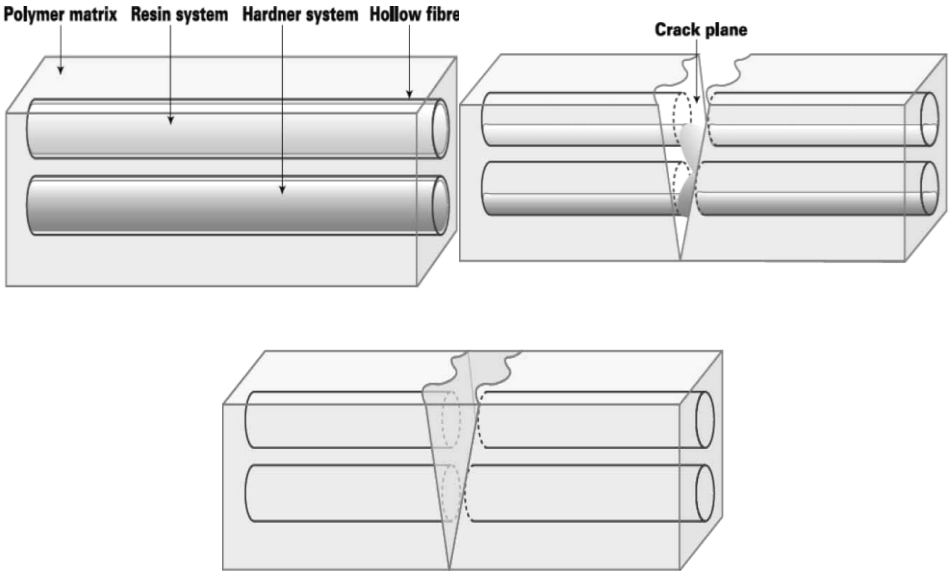

Figure1.2: Self-healing concept using hollow fibers or tubes

1.3.1. Three-dimensional micro-vascular networks

In conventional extrinsic self-healing composites, it is hard to perform repeated healing, because rupture of the embedded healant-loaded containers would lead to depletion of the healing agent after the first damage. To overcome this difficulty,Toohey *et al*. proposed a self-healing system consisting of a three-dimensional microvascular network capable of autonomously repairing repeated damage events [4].

- **Vascular materials**, the healing agent is stored in hollow channels or fibers until damage ruptures the vasculature and releases the healing agent.

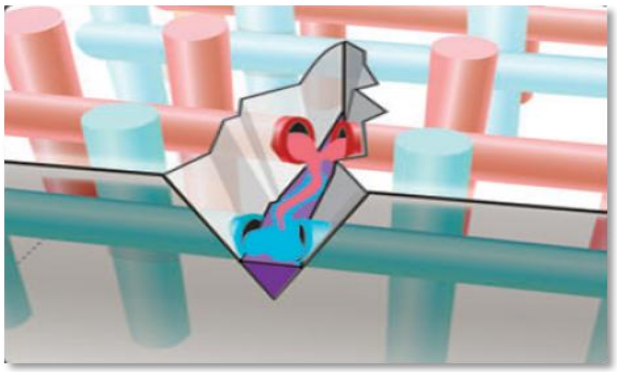

Figure 1.3: Vascular based self-healing materials

- **Disadvantages of vascular materials**

Vascular approaches hold great promise for healing large damage volumes over multiple damage events, but their integration in existing material systems is challenging.

1.3.2. Self-healing in materials containing healant loaded microcapsules

The principle of this approach resembles the afore mentioned pipelines, but the containers for storing the healing agent are replaced by fragile microcapsules. Because the technique of microencapsulation has seen rapid advances since its emergence in 1950s [5] and mass production of microcapsules can be industrialized; microcapsule based self-healing composites exhibit potential to become a reality in the future[6].

- **Capsule-based self-healing**

In capsule-based self-healing materials, the healing agent is stored in capsules until they are ruptured by damage. In the event of rupture, the self-healing mechanism is triggered through the release and reaction of the healing agent in the region of damage. After release, the local healing agent is depleted, leading to only a singular local healing event. For example, UF, MF/MUF, and PU capsules used for self-healing which have shown ability to survive processing conditions in common thermoset resin matrices and composite manufacturing processes and that have been prepared at multiple size scales.

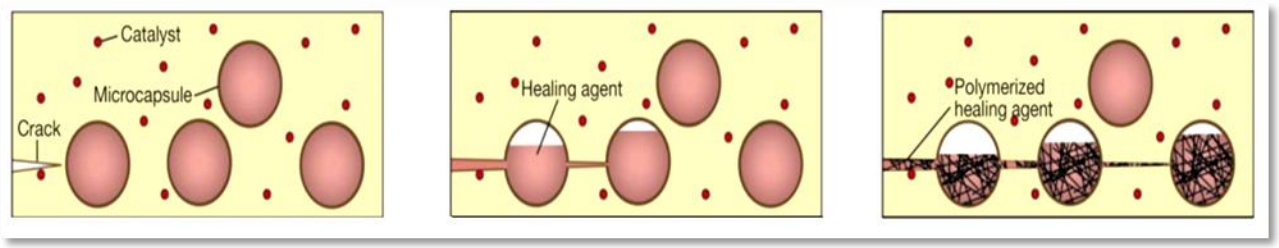

Figure 1.4: Capsule-based self-healing materials

- **Disadvantages of capsule-based self-healing materials**

Capsule-based approaches are easily integrated in most polymer systems, but their function is locally depleted after a single damage event.

1.4 Previous Work

Since there has been so much demand for autonomic healing in artificial materials, there have been a number of previous attempts to introduce self-healing functionality to polymers glasses and concrete[7]. It has been known for some time that when a thermoplastic polymer such as poly(methyl methacrylate) (PMMA) is damaged, it can be repaired by heat or solvent treatments that causes diffusion of the thermoplastic polymer across the crack plane. Basically, solvent or heat brings the sample above its glass transition temperature and the polymer chains can diffuse and entangle[8]. However, these kinds of treatments that require external intervention such as heat, pressure, ultra violet radiation, or solvent are not descriptive of a self-healing system. Moreover, it is necessary to know that there is damage in the sample in the first place prior to external treatment of the damaged region.

A more advanced system, using a thermally re-mendable cross-linked polymeric material, for a thermoset polymer was recently reported by Chen and Wudl [9]. This material can undergo repeated healing by reversible Diels-Alder reaction with multi-dienes and multi-dineophiles. It was reported that about 30% of the covalent bonds can be reversibly disconnected and reconnected by temperature change, so that it can heal the fracture of samples multiple times without a catalyst, additional monomer, or special surface treatment. However, this system requires a specially synthesized monomer, and in addition, a high temperature treatment of above 120°C. Since external intervention is required, this again, is not truly autonomic healing. An example of true self-healing materials is a system composed of an encapsulated healing agent in a matrix polymer. In this system, the healing reaction is only triggered when the encapsulated healing agent is released by a mechanical damage event. The first study of this kind used macroscale glass tubes which contained cyanoacrylate or two-part epoxy resin in an epoxy matrix. It was proved that encapsulated healing agents have the possibility for self-healing in the cracked damage by polymerization of the released healing agent from the glass capillary. However, making glass tubes containing monomers and distributing them inside a matrix is a

difficult and time-consuming process, which renders this technique practically difficult. Self-healing with an encapsulated healing agent becomes realizable when a microencapsulated monomer, which can be dispersed through the matrix, is used. Microcapsules enables self-healing polymer mass production, even distribution, and effective healing in the case of relatively small cracks inside a matrix. The problem was insufficient microcapsule rupture by crack invasion and incomplete polymerization of the monomer by the initiator[10].

A breakthrough in self-healing research was developed by White et al., which induced living ring opening metathesis polymerization (ROMP) of dicyclopentadiene (DCPD) in the presence of ruthenium (Ru) based Grubbs' catalyst [11]. The healing agent, DCPD, is microencapsulated by in situ polymerization of urea-formaldehyde, which forms a shell outside of the DCPD liquid droplet. The size of microcapsules is determined by mechanical stirring speeds, typically 10-1000 μm in the range of 200-2000 rpm[12]. These microcapsules effectively deliver the healing agent to the cracked plane, induce polymerization by contact with the catalyst, and finally seal the damage. The healing efficiency of this system, calculated by the relative ratio of healed toughness to virgin toughness, was reported as 75% [11]. However, this self-healing polymer needs relatively large amount (2.5 wt %) of embedded Grubbs' catalyst, which is quite expensive. A small amount of unprotected Grubbs' catalyst could not accomplish successful healing because of poor dispersion of the catalyst in the matrix, which causes exposure of only a few large particles on the crack plane. Moreover, Grubbs' catalyst is susceptible to deactivation by contact with the amine curing agent used for epoxy matrix polymerization. Rule et al. used Grubbs' catalyst encapsulated microspheres with paraffin wax to protect the catalyst from the amine curing agent [13]. Catalyst containing microspheres are synthesized by mixing molten wax and Grubbs's catalyst in hot water with ethylene-maleic anhydride copolymer as a surfactant under mechanical stirring, followed by quenching in ice water. When a crack propagates into a matrix, the healing agent released from the microcapsules dissolves the wax and induces the healing

reaction [14]. Wax-protected catalyst microspheres can also improve the dispersion property of the catalyst in the matrix, and consequently induce the uniform exposure of the catalyst to the cracked plane [13,14]. The healing efficiency calculated by the ratio of internal work between the healed sample and the virgin sample is reported as a maximum 93% [13]. Although less catalyst is required by wax protected catalyst microspheres, this system still uses Grubbs' catalyst, which has some limitations.

1.5 Microencapsulation

Microencapsulation is a process by which very tiny droplets or particles of liquid or solid material are surrounded or coated with a continuous film of polymeric material for the purpose of shielding the active ingredient from the surrounding environment. Microencapsulation provides the means of converting liquids to solids, of altering colloidal and surface properties, of providing environmental protection and of controlling the release characteristics or availability of coated materials. All three states i.e. solid, liquid and gases, may be encapsulated and affect the size and shape of the capsules. If a solid or a crystalline material is used as the core, the resultant capsule may be irregularly shaped. However, if the core material is a liquid, simple spherical capsules, containing a single droplet of encapsulate, may be formed.

1.5.1. Core Materials

The core material, defined as the specific material to be coated, can be liquid or solid in nature. The composition of the core material can be varied, as the liquid core can include dispersed and/or dissolved materials. The solid core can be active constituents, stabilizers, diluents, excipients, and release-rate retardants or accelerators. The ability to vary the core material composition provides definite flexibility and utilization of this characteristic often allows effectual design and development of the desired microcapsule properties.

- **UNSATURATED POLYESTER AS A HEALING AGENT**

Sriram and Rule described the required properties of a healing agent for self-healing material. Basically, unique characteristics for self-healing materials are: long period of activity and stability, good deliverability, high reactivity, minimal shrinkage, and no negative effect on physical properties of materials either before or after healing[10,14]. Moreover, Rule also pointed out limitations of self-healing chemistry using DCPD and Grubbs' catalyst. Those drawbacks are: a slow rate of healing, a narrow operating temperature range, the high cost of Grubbs' catalyst, the severely limited availability of Grubbs' catalyst, and a large extent of pre-healing damage. Some of these limitations are improved by microencapsulated Grubbs' catalyst with paraffin wax [13]. However, to devise a more practical material, it is necessary to access a chemistry which is economically viable. Commonly used healing agents in literature are DCPD[12], Epoxy[15] and PDMS[16]. For the present work, USP was chosen as a healing agent in our study and we made much progress in eliminating previously mentioned limitations. Unsaturated thermosetting polyester (USP) is one of the most widely used fiber-reinforced composite matrix material, its popularity arising from its excellent mechanical properties, chemical resistance, low cost, ease of processing and excellent fiber wettability[17]. Conventional UPRs are primarily solutions of unsaturated polyesters with a diluent, usually styrene, and the curing process results in the linking of polyesters chains through poly (styrene) linkages at the unsaturated sites, thereby forming an amorphous three-dimensional molecular structure. However, this cross-linked network is inherently brittle, which restricts its usage in highly demanding applications. Due to the presence of styrene, USP can undergo free radical polymerisation in the presence of suitable initiators. In the view of this property of USP, we have encapsulated USP in urea-formaldehyde shell and dispersed the resulting microcapsules in varying amounts (10-30% w/w) within epoxy matrix to prepare self-healing composites. The self-healing efficiencies of the developed composites have been evaluated as the ratio of impact strengths of healed to virgin

specimen[6]. To decrease the healing temperature we have also investigated the effect of introducing a free radical initiator (AIBN, 1% w/w of microcapsules) in the matrix.

1.5.2. Shell material or Coat material

The shell or coat is the envelope which is made of a continuous, porous or nonporous, polymeric phase. It covers or protects the core material. It is important to note that the microcapsule shell wall material has to be chosen judiciously and presently, urea-formaldehyde (UF) and melamine formaldehyde (MF) are most commonly employed, primarily because of their reasonable cost, adequate strength and long shelf-life.

- **UREA-FORMALDEHYDE AS A SHELL MATERIAL**

Urea-formaldehyde resins are most important commercially prepared amino resins. U-F resins are relatively cheaper than MF, light in color, lack in odor, exhibit good electrical insulation properties with particularly good resistance to electrical tracking. U-F resin is usually prepared by two step process.

1.6. TECHNIQUES FOR THE PREPARATION OF MICROCAPSULES

There are various techniques are available for the encapsulation of core materials. Broadly, the methods are divided into two types these are:

1.6.1. PHYSICO-MECHANICAL PROCESS

1.6.1.1. Air-suspension coating:

Air-suspension coating, first described by Professor Dale Erwin Wurster at the University of Wisconsin in 1959.In this process, the particulate solid core material is dispersed into the supporting air stream, which are coated with polymers in a volatile solvent leaving a very thin layer of polymer on them. This process is repeated several hundred times until the required parameters such as coating thickness, etc., are achieved. The air stream which supports the

particles also helps to dry them, and the rate of drying is directly proportional to the temperature of the air stream which can be modified to further affect the properties of the coating.

The re-circulation of the particles in the coating zone portion is effected by the design of the chamber and its operating parameters. The coating chamber is arranged such that the particles pass upwards through the coating zone, then disperse into slower moving air and sink back to the base of the coating chamber, making repeated passes through the coating zone until the desired thickness of coating is achieved.

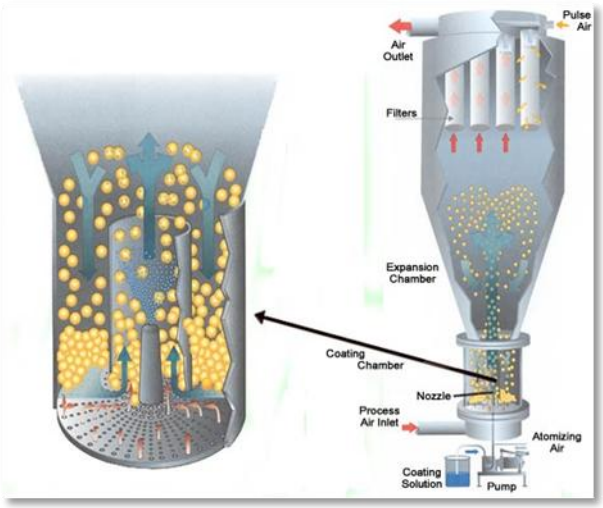

Figure1.5: Air-suspension coating

1.6.1.2. Pan coating:

The pan coating process, widely used in the pharmaceutical industry, is among the oldest industrial procedures for forming small, coated particles or tablets. The particles are tumbled in a pan or other device while the coating material is applied slowly. Solid particles greater than 600 microns in size are generally considered as a prerequisite for effective coating, and the process has been extensively employed for the preparation of controlled - release beads. Unlike many other microencapsulation processes, the process tends itself to great flexibility in formulation of coating. Core material may contain wide range of additive may serve to modify release properties of formulation.

Figure1.6: Pan Coating

1.6.1.3. Spray-drying:

Spray drying is a mechanical microencapsulation method developed in the 1930s. An emulsion is prepared by dispersing the core material, usually an oil or active ingredient immiscible with water; into a concentrated solution of wall material until the desired size of oil droplets are attained. The resultant emulsion is atomized into a spray of droplets by pumping the slurry through a rotating disc into the heated compartment of a spray drier. There, the solvent water in the emulsion is evaporated, yielding dried capsules of variable shape containing scattered drops of core material. The capsules are collected through continuous discharge from the spray drying chamber. This method can also be used to dry small microencapsulated materials from aqueous slurry that are produced by chemical methods.

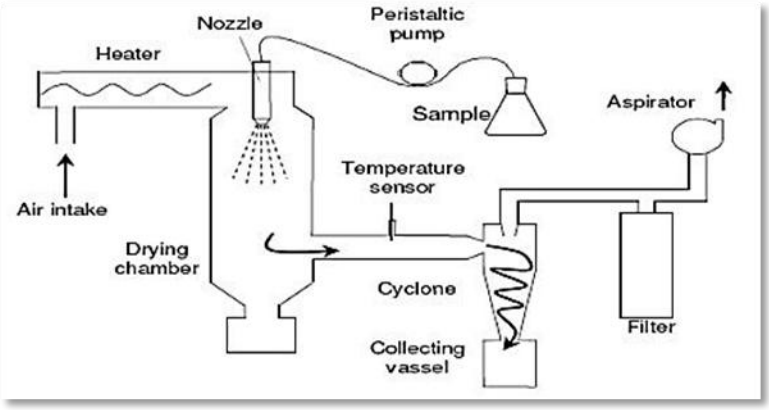

Figure1.7: Schematic illustrating the process of micro-encapsulation by spray-drying

1.6.3. CHEMICAL METHOD

1.6.3.1 *In Situ* Polymerization

In situ polymerization is a chemical encapsulation technique very similar to interfacial polymerization. *In situ* polymerization requires that the monomers for the shell creation are soluble in continuous, often water phase, whereas the core material is immiscible with water and presents in the form of emulsion. In many cases, copolymers are used in order to stabilize emulsion and enhance deposition of the shell material. In a few microencapsulation processes, direct polymerization of a single monomer is carried out on the particle surface. Like Interfacial polymerization (IFP) the capsule shell formation occurs because of polymerization of monomers added to the encapsulation reactor. In this process no reactive agents are added to the core material, polymerization occurs exclusively in the continuous phase and on the continuous phase side of the interface formed by the dispersed core material and continuous phase. The distinguishing characteristic of in situ polymerization is that no reactants are included in the core material. All polymerization occurs in the continuous phase, rather than on both sides of the interface between the continuous phase and the core material, as in IFP. Examples of this method include urea-formaldehyde (UF) and melamine formaldehyde (MF) encapsulation systems.

1.6.3.2. Emulsion Polymerization Technique

Emulsion polymerization is a type of heterogeneous radical polymerization that starts with an emulsion incorporating water, monomer, and surfactant. Most common type of emulsion polymerization is an oil-in-water emulsion, in which droplets of monomer (oily phase) are emulsified with surfactants in a continuous phase of water. According to this technique unsaturated polyester is added drop wise to the stirred aqueous polymerization medium containing the material to be encapsulated (core material) and a suitable emulsifier·

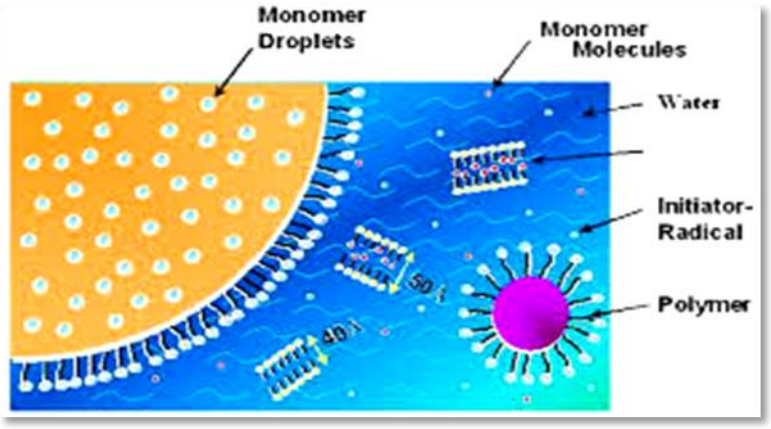

Figure1.8: Emulsion Polymerization technique

The polymerization begins and initially produced polymer molecules precipitate in the aqueous medium to form primary nuclei. As the polymerization proceeds, these nuclei grow gradually and simultaneously entrap the core material to form the final microcapsules. Generally lipophilic materials (insoluble or scarcely soluble in water) are more suitable for encapsulation by this technique. Unsaturated polyester loaded urea formaldehyde microcapsules have been synthesized by using this technique.

For self-healing materials, the most common encapsulation techniques are in situ, interfacial, and meltable dispersion. In situ and interfacial encapsulations proceed by reaction of urea-formaldehyde (UF), melamine-formaldehyde (MF), polystyrene.

1.7 Curing agents for USP

- Methyl ethyl ketone peroxide (**MEKP)**

MEKP is organic peroxide used for curing resins, particularly polyester and vinyl ester resins. MEKP starts the chemical reaction of the resin with the styrene monomer (present as a diluent in the resin) allowing cross-links to form between them. These cross-links act as braces, joining the components in the liquid resin together. When some of the cross-links have formed, the resin forms a gel, and as the cross-linking proceeds, the resin forms a solid and is said to have been "cured".

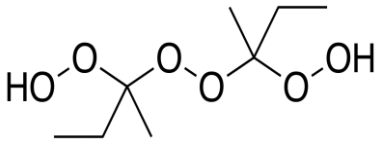

Methylethylketoneperoxide (**MEKP)**

- 2, 2'-azobis (isobutyronitrile) (**AIBN)**

2, 2'-Azobisisobutyronitrile (AIBN) is the most important initiators in the azo compounds which is commonly used at 50–70ºC. It is a white powder which is soluble in alcohol and common organic solvents but is insoluble in water. These radicals can initiate free radical polymerizations and other radical-induced reactions. For instance, a mixture of styrene and maleic anhydride in toluene will react if heated, forming the copolymer upon addition of AIBN. AIBN is safer to use than benzoyl peroxide (another radical initiator) because the risk of explosion is far less. However, it is still considered as an explosive compound, decomposing above 65°C.

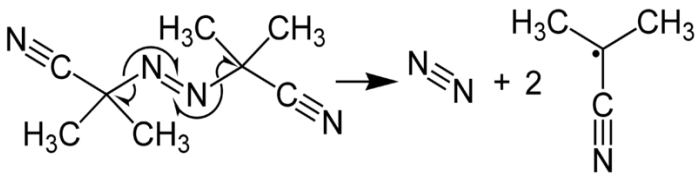

Scheme 1: Mechanism of AIBN decomposition

This colorless liquid has a characteristic sweet smell and is used in glues, nail polish removers, decaffeinating tea and coffee, and cigarettes. Ethyl acetate is the ester of ethanol and acetic acid; it is manufactured on a large scale for use as a solvent.

1.7.1. Curing of unsaturated polyesters

Unsaturated polyester (USP) is highly viscous in nature. To reduce the viscosity of unsaturated polyester (USP) ethyl acetate is mixed in the 1:1 w/w ratio. Ethyl acetate is used primarily as a solvent and diluent, being favored because of its low cost, low toxicity, and agreeable odor. For example, it is commonly used to clean circuit boards and in some nail varnish removers.[1,18]

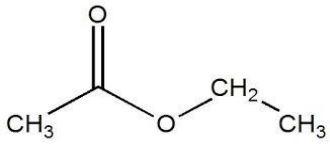

Ethyl acetate

It is also used in paints as an activator or hardener. Ethyl acetate is present in perfumes, and fruits. In perfumes, it evaporates quickly, leaving only the scent of the perfume on the skin. In order to obtain a rigid, structural material the pre-polymer styrene solution is cross-linked by the user into a rigid thermoset in a free radical copolymerization between the styrene monomer and the polyester double bonds originating from the unsaturated di-carboxylic acid.

The co-polymerization is initiated by azo compounds. The cross-linking reaction is a highly exothermic reaction, and the temperature can increase up to 100-200°C, depending on the resin composition, laminate thickness, and the initiator system. The cross-linking reaction is not complete, however. Even when the final solid state is achieved there will be unreacted styrene monomers and double bonds left. This residual reactivity can be removed by post-curing simply by heating at a temperature above the glass transition temperature of the cross-linked unsaturated polyester. This process of network formation is often named in the literature as curing, and the degree of cure is taken as the cross-linking density.

The preparation of unsaturated polyester is presented in **Scheme 2**

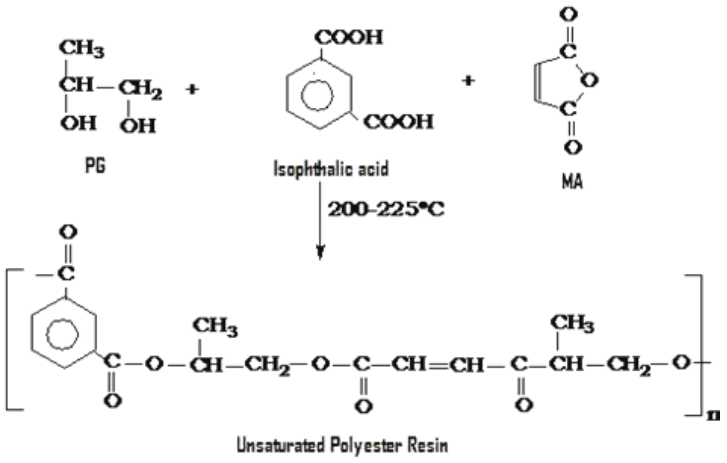

The cross-linked structure of cured polyester is presented below

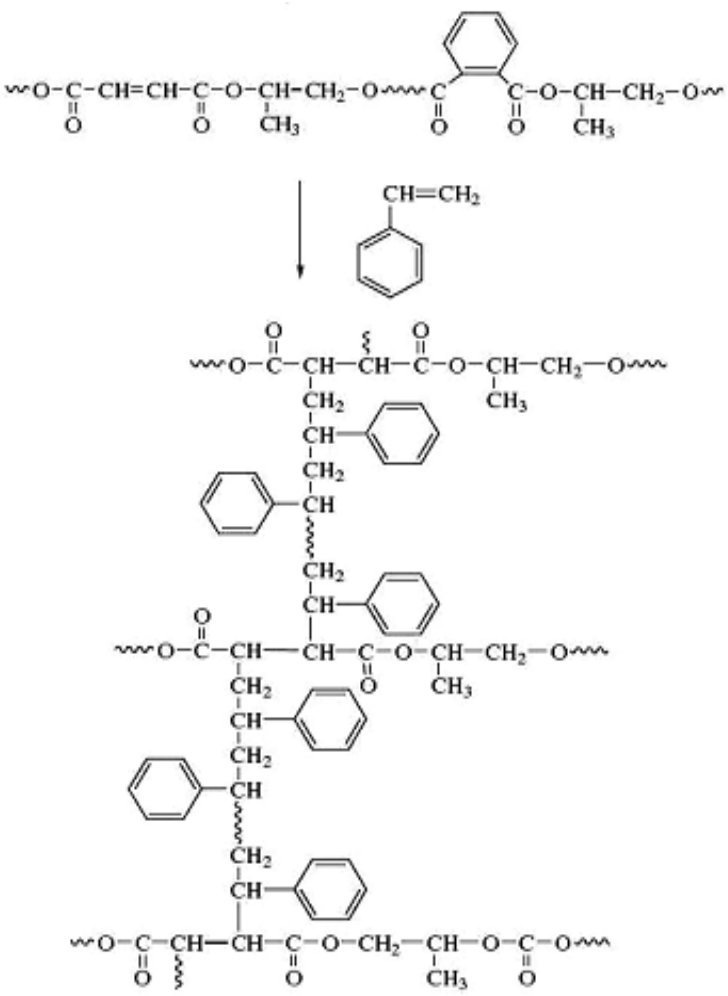

Scheme 2: Polyester Resin Scheme with Cross linking[19]

1.8.1. Healing Efficiency

Healing can refer to the recovery of properties like fracture toughness, tensile strength, surface smoothness, barrier properties and even molecular weight. In general self-healing efficiency can be calculated as

$$\text{Healing Efficiency} = 100 \times \frac{\text{Property value}_{\text{Healed}}}{\text{Property value}_{\text{Initial}}}$$

1.8.2. Evaluation of self-healing efficiency

A compact, constant stress intensity factor, side grooved, tapered double-cantilever-beam (T-DCB) specimen has been designed for measuring elevated temperature creep and fatigue crack growth rates. Crack healing efficiency (η) was assessed as ability to recover fracture toughness at the monotonic conditions and defined as the ratio of the fracture toughness of healed $K_{IC,\ healed}$ and virgin $K_{IC,\ virgin}$ materials:

$$\eta = \frac{K_{Ic_{healed}}}{K_{Ic_{virgin}}}$$

A tapered double-cantilever beam (TDCB) test was used in order to find the fracture toughness values. The geometry of TDCB specimen (Figure 1.9) ensures a controlled crack growth across the centre of a brittle sample and makes the fracture toughness to be independent of the crack length.

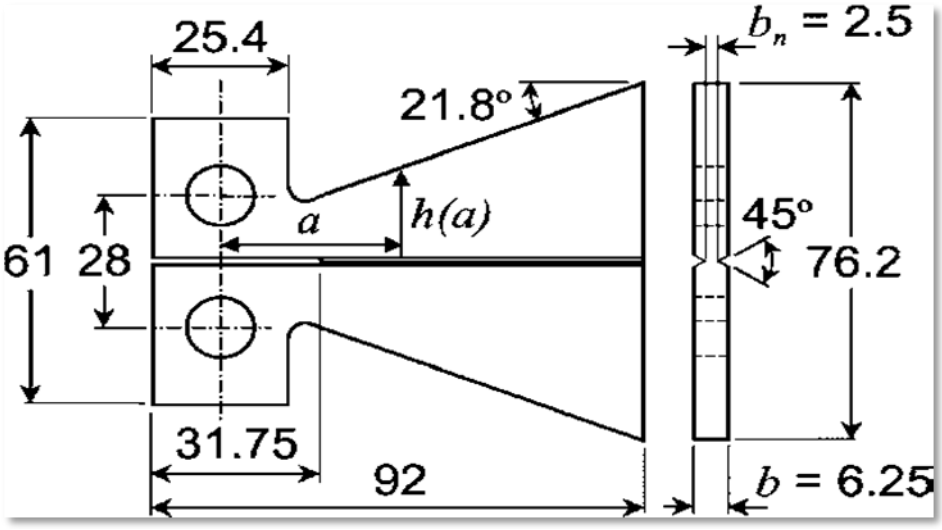

Figure 1.9: Tappered double-cantilever beam (TDCB) geometry [20]. Note: all dimensions in mm.

Thus, in order to calculate fracture toughness of TDCB specimen only the critical fracture load (*Pc)* needs to be measured and geometric terms need to be known [20]. The healing efficiency can be determined as

$$\eta = \frac{P_{c_{healed}}}{P_{c_{virgin}}}$$

Capability of the self-healing system to retard fatigue crack growth can be assessed under cyclic loading conditions as the fatigue life-extension:

$$\lambda = \frac{N_{healed} - N_{control}}{N_{control}}$$

Where N_{healed} is the total number of cycles to failure for the self-healing sample and $N_{control}$ is the total number of cycles to failure for a similar sample without healing [20].

1.8.3. Self-healing efficiency by impact strength measurements

Self-Healing efficiencies can also be calculated as a ratio of healed to virgin impact strength. For this the virgin specimen is impacted apart, and then the broken parts are recombined. The healed specimen is again subjected to impact loading and impact strength is measured.[21] The healing efficiency can be determined as

η = Impact strength healed specimen / Impact strength virgin specimen

1.8.4. Application

Self-healing materials are no more an illusion and we are not far away from the days when manmade materials can restore their structural integrity in case of a failure. For example, the cracks in buildings can close on their own or the scratches on car bodies can recover their

original shiny appearance by itself. Virtually, all materials are susceptible to natural or artificial degradation and deteriorate with time. In the case of structural materials the long-time degradation process leads to microcracks that causes a failure. Thus, repairing is indispensable to enhance reliability and lifetime of materials. Though scientists are inspired by the natural process of blood clotting or repairing of fractured bones, incorporating the same concept into engineering materials is far from reality due to the complex nature of the healing processes in human bodies or other animals. However, the recent announcement from Nissan on the commercial release of scratch healing paints for use on car bodies has gained public interest on such a wonderful property of materials.

Other potential application are:

- Microelectronics Packaging
- Automotive Coatings
- Hip Joint Replacement
- Helicopter Rotor Blade

1.9 Project aims and objectives

This project aims at developing a novel approach towards the formation of urea formaldehyde microcapsules which is encapsulated with unsaturated polyester.

More specifically, the objectives of this research are:

- To prepare and characterize unsaturated polyester encapsulated urea formaldehyde microcapsules.
- To prepare epoxy composites containing developed microcapsules.
- To investigate the effect of increasing loading of the microcapsules on the impact strength of the composites.

- To evaluate the self- healing efficiency of the composites
- To study the effect of increasing loading of microcapsules on self-healing efficiency of the composites.

CHAPTER 2: EXPERIMENTAL

2.1. Introduction

The experimental work was carried out in two different stages. The first stage deals with the preparation of microcapsules containing different healing agents, like unsaturated polyester and cycloaliphatic epoxy. The microencapsulation was achieved by both physical evaporation technique as well as emulsion polymerization process, which has been discussed in this chapter. The various techniques used for characterization of microcapsules are also described under various sub-sections. The second part deals with the applicability of the developed microcapsules in the area of self-healing. The details of composition prepared along with techniques for self- healing efficiency determination are also discussed.

Experimental

2.2. Materials

Epoxy monomer (Araldite CY 230; epoxy equivalent 200 eq/g) (as healing agent as well as the matrix) as well as triethylenetetramine (TETA) based curing agent (HY 951; amine content (32 eq/kg) was purchased from Ciba Geigy, and used as received. Urea, formalin (37% formaldehyde in water), citric acid, was obtained from CDH. EMA (Sigma Aldrich) was used without any further purification. For the preparation of the latent hardener, 2-MeIm (97%, Sigma Aldrich) and $CuCl_2.2H_2O$ (A.R., CDH), were used. Isophthalic acid based unsaturated polyester resin (USP RPL211) with a styrene content of 32% was kindly provided by Revex, (Delhi, India).Distilled water was used throughout the course of this work.

2.2.1. Preparation of USP encapsulated Polystyrene microcapsules

USP was encapsulated in PS microcapsules by solvent evaporation technique using the procedure reported in the literature[22]. A solution of USP in chloroform (20% w/v) was added drop wise to 100 mL aqueous PVA solution (2.5% w/v) under continuous stirring (500 rpm). Separately, a solution of polystyrene (PS) in chloroform (2-10% w/v) was injected through a hypodermic syringe into the reaction vessel maintained at 60°C. The stirring rate was varied from 400-600 rpm to investigate its effect on the particle dimensions. Post-evaporation of

chloroform, the reaction mixture was cooled, and the USP encapsulated PS microcapsules were filtered and washed repeatedly with water followed by drying under vacuum.

2.2.2. Preparation of epoxy encapsulated urea-formaldehyde microcapsules

Epoxy encapsulated microcapsules were prepared by an in situ oil-in-water (O/W) emulsion polymerization route using the procedure reported in the literature.[1] For encapsulation, 100 mL distilled water and 2.5 ml EMA solution (2.5 % w/v) was taken into a 500ml capacity beaker with stirring at room temperature (~450 rpm). Then to this solution, 2.5 g urea, 0.25 g ammonium chloride and 0.25 g resorcinol was added and stirred to dissolve the solid wall-forming materials. After dissolution pH was decreased to 3-3.5 with citric acid aqueous solution (5% w/v). Subsequently, ~60 ml of the healing agent solution (epoxy: ethyl acetate::ratio 1:1 w/w) was slowly added over a period of 20 min while maintaining a stirring speed of ~350 rpm. Subsequently, requisite amount (6.33 g) of formaldehyde solution (37 %) was added, and the temperature was increased to 50-55°C, while maintaining a stirring speed of ~350 rpm. The reaction was allowed to proceed for 4 h, followed by filtration and air drying for 24 h.

2.2.3. Preparation of unsaturated polyester encapsulated urea-formaldehyde microcapsules

USP encapsulated microcapsules were prepared by an in situ oil-in-water (O/W) emulsion polymerization route using the procedure reported in the literature[1]. For unsaturated polyester encapsulation, 100 mL distilled water was introduced into a 500ml capacity beaker containing 25 ml EMA solution (2.5 % w/v) while stirring at room temperature (~450 rpm). To this solution, 2.5 g urea, 0.25 g ammonium chloride and 0.25 g resorcinol was added. After dissolution of the solid wall-forming materials, pH was decreased to 3-3.5 with citric acid aqueous solution (5% w/v). Subsequently, ~60 ml of the healing agent solution (unsaturated polyester resin: ethyl acetate::ratio 1:1 w/w) was slowly added over a period of 20 min while maintaining a stirring speed of ~350 rpm. Subsequently, requisite amount (6.33 g) of formaldehyde solution (37 %)

was added, and the temperature was increased to 50-55°C, while maintaining a stirring speed of ~350 rpm. The reaction was allowed to proceed for 4 h, followed by filtration and air drying for 24 h.

2.3 Core Content determination

The extent of encapsulation in the microcapsules was determined by acetone extraction method as per the reported procedure.[15] For this purpose, an accurately weighed amount of microcapsules (M_{mc}) was crushed to release the encapsulated healing agent. The resulting powder was then washed with acetone, filtered, dried and weighed (M_{shell}). The core content was determined gravimetrically as the ratio of encapsulated mass of epoxy (M_{mc} - M_{shell}) to the initial mass of the microcapsules (M_{mc}).

2.4 Preparation of Latent curing agent for epoxy

$CuCl_2.2H_2O$ (5.6 g) was dissolved in 25 ml methanol and 2-methylimidazole (10.7 g) was dissolved in 12.5 ml of water. Both the methanolic solutions were then mixed and stirred for about 3-4 h. The above mixture is then diluted by addition of 75 ml acetone, resulting into the precipitation of the complex. The precipitate was filtered, washed and then dried.

2.5 Characterization

FTIR spectra of samples were recorded in the wavelength range 4000 - 600 cm^{-1} using a Thermo Fisher FTIR (NICOLET 8700) analyser with an attenuated total reflectance (ATR) crystal accessory. The thermal behavior was investigated using Perkin Elmer Diamond STG-DTA under N_2 atmosphere in the temperature range 50-800 °C. A heating rate of 10 °C/min and sample mass of 5.0 ± 0.5 mg was used for each experiment. Izod single-notched impact test was used to measure the self-healing efficiency as the ratio of impact strength of healed specimen to the impact strength of virgin.The notched Izod impact strength of the specimens was determined as per ASTM D 256 using an impact strength testing machine (International Equipments, India).

Self-healing efficiency was determined as the ratio of impact strengths of healed sample to virgin sample.[21] For each composition, at least five identical specimens were tested and the average results along with the standard deviation have been reported. The surface morphology of samples was studied using a Scanning Electron Microscope (Zeiss EVO MA15) under an acceleration voltage of 20 kV. Samples were mounted on aluminium stubs and sputter-coated with gold and palladium (10 nm) using a sputter coater (Quorum-SC7620) operating at 10-12 mA for 120 s.

2.5.1. Scanning electron microscopy

The surface morphology of samples was studied using a Scanning Electron Microscope (Zeiss EVO MA15) under an acceleration voltage of 20 kV. Samples were mounted on aluminium stubs and sputter-coated with gold and palladium (10 nm) using a sputter coater (Quorum-SC7620) operating at 10-12 mA for 120 s. The core shell structure of the epoxy coated PDMS microspheres was also confirmed using EDX. For this purpose, a representative epoxy coated microsphere was cut with a sharp razor blade and carefully mounted on a stub and sputter coated with gold. The elemental composition in the core and shell region was determined using an energy dispersion analyser (EDS).

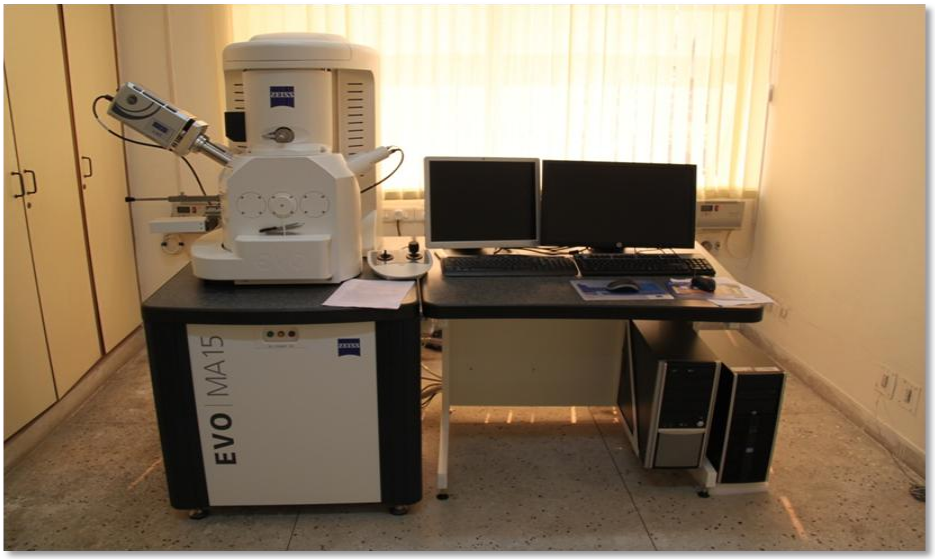

Figure 2.1: Scanning electron microscope

Principle:

Accelerated electrons in an SEM carry significant amounts of kinetic energy, and this energy is dissipated as a variety of signals produced by electron-sample interactions when the incident electrons are decelerated in the solid sample. These signals include secondary electrons (that produce SEM images), backscattered electrons (BSE), diffracted backscattered electrons (EBSD that are used to determine crystal structures and orientations of minerals), photons (characteristic X-rays that are used for elemental analysis and continuum X-rays), visible light (cathodoluminescence--CL), and heat. Secondary electrons and backscattered electrons are commonly used for imaging samples: secondary electrons are most valuable for showing morphology and topography on samples and backscattered electrons are most valuable for illustrating contrasts in composition in multiphase samples (i.e. for rapid phase discrimination).

Instrumentation:

Essential components of all SEMs include the following:

- Electron Source ("Gun")
- Electron Lenses
- Sample Stage
- Detectors for all signals of interest
- Display / Data output devices
- Infrastructure Requirements:
  - o Power Supply
  - o Vacuum System
  - o Cooling system
  - o Vibration-free floor
  - o Room free of ambient magnetic and electric fields

SEMs always have at least one detector (usually a secondary electron detector), and most have additional detectors. The specific capabilities of a particular instrument are critically dependent on which detectors it accommodates.

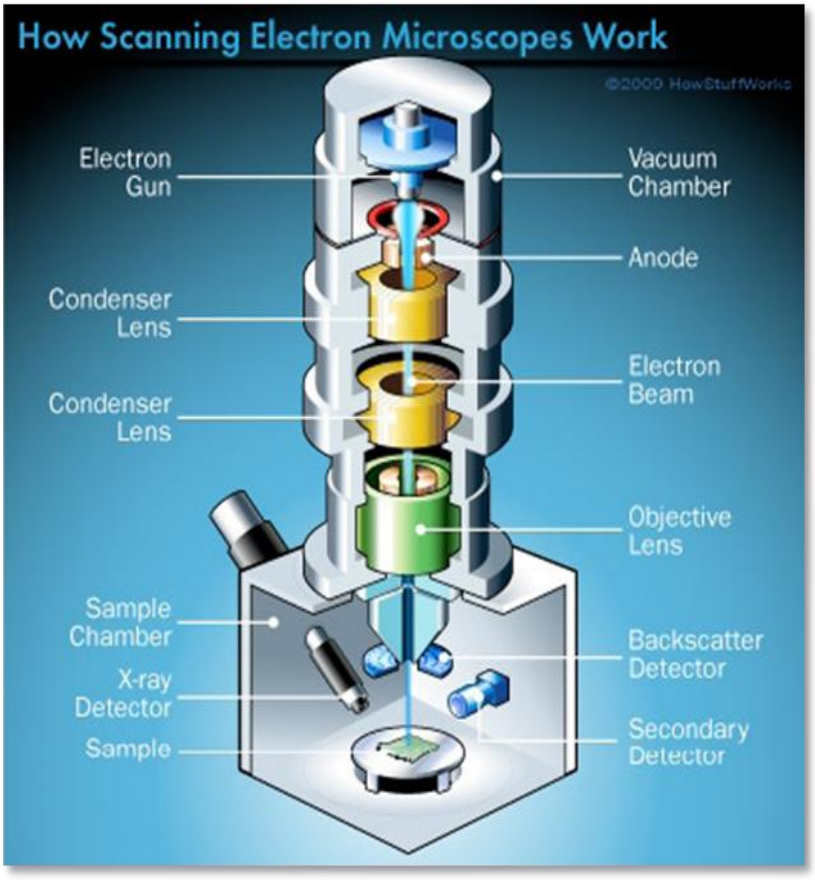

Figure 2.2 Schematic diagram of the working of a scanning electron microscope

2.5.2. ATR-FTIR

FTIR spectra of samples were recorded in the range 4000 - 600 cm^{-1} using Fourier Transform Infrared (FTIR) spectroscopy on a Thermo Fisher FTIR (NICOLET 8700) analyser with an attenuated total reflectance (ATR) crystal accessory.

Figure 2.3: ATR-FTIR

Principle

An attenuated total reflection accessory operates by measuring the changes that occur in a totally internally reflected infrared beam when the beam comes into contact with a sample. An infrared beam is directed on to an optically dense crystal with a high refractive index at a certain angle. This internal reflectance creates an evanescent wave that extends beyond the surface of the crystal into the sample held in contact with the crystal. It can be easier to think of this evanescent wave as a bubble of infrared that sits on the surface of the crystal. This evanescent wave protrudes only a few microns (0.5-5μ) beyond the crystal surface and into the sample. Consequently, there must be good contact between the sample and the crystal surface. In regions of the infrared spectrum where the sample absorbs energy, the evanescent wave will be attenuated or altered. The attenuated energy from each evanescent wave is passed back to the IR beam, which then exits the opposite end of the crystal and is passed to the detect or in the IR spectrometer. The system then generates an infrared spectrum.

2.5.3. Thermal Analysis

The thermal behavior was investigated using Perkin Elmer Diamond STG-DTA under air atmosphere (flow rate = 50 ml/min) in the temperature range 50-800°C. A heating rate of 10°C/min and sample mass of 5.0 ± 0.5 mg was used for each experiment.

Figure 2.4 Thermogravimetric analysis

Principle

Thermogravimetric analysis (TGA) is based on the measurement of mass loss of material as a function of temperature. In thermogravimetry, a continuous graph of mass change against temperature is obtained when a substance is heated at a uniform rate or kept at constant temperature. The measurement can be performed in air or inert atmosphere, depending on the requirement and the weight is recorded as a function of increasing temperature. A plot of mass change versus temperature (T) is referred to as the thermogravimetric curve (TG curve).

2.5.4. Differential Scanning Calorimetry (DSC)

Differential Scanning Calorimetry, or DSC, is a thermal analysis technique that looks at how a material's heat capacity (Cp) is changed by temperature. A sample of known mass is heated or cooled and the changes in its heat capacity are tracked as changes in the heat flow. This allows the detection of transitions such as melts, glass transitions, phase changes, and curing. Because of this flexibility, since most materials exhibit some sort of transitions, DSC is used in many industries, including pharmaceuticals, polymers, food, paper, printing, manufacturing, agriculture, semiconductors, and electronics.

The biggest advantage of DSC is the ease and speed with which it can be used to see transitions in materials. If you work with polymeric materials of any type, the glass transition is important to understanding your material. In liquid crystals, metals, pharmaceuticals, and pure organics, you can see phase changes or polymorphs and study the degree of purity in materials. If you are processing or distilling materials, knowledge of a material's heat capacity and heat content change (called enthalpy) can be used to estimate how efficiently your process is operating.

For these reasons, DSC is the most common thermal analysis technique and is found in many analytical, process control, quality assurance, and R&D laboratories. The Q20 Series (Q20, AQ20, Q 20P) are cost-effective, easy-to-use, general-purpose DSC modules, with calorimetric performance equal superior to many competitive research-grade models. These are entry-level instruments not based on performance, but on available options.

The Q20 family is ideal for research, teaching, and quality control applications that require a rugged, reliable, basic DSC. The AQ20 is designed for unattended analysis of up to 50 samples in a random or sequential manner. The Q20 and Auto Q20 include dual digital mass flow controllers. The Q20P is designed for studies of pressure sensitive materials, or samples that may volatilize on heating. For dynamic DSC scans, samples (10 ±2 mg) were sealed in aluminum pans, and heated from 0-250°C at 10°C /min.

Figure 2.5 Differential Scanning Calorimetry (DSC) Q20 Series

Principle

When a sample undergoes a physical transformation such as a phase transition, more or less heat will need to flow to it than to the reference (typically an empty sample pan) to maintain both at the same temperature. Whether more or less heat must flow to the sample depends on whether the process is exothermic or endothermic. For example, as a solid sample melts to a liquid it will require more heat flowing to the sample to increase its temperature at the same rate as the reference. This is due to the absorption of heat by the sample as it undergoes the endothermic phase transition from solid to liquid. Likewise, as the sample undergoes exothermic processes (such as crystallization) less heat is required to raise the sample temperature. By observing the difference in heat flow between the sample and reference, differential scanning calorimeters are able to measure the amount of heat absorbed or released during such transitions. DSC may also be used to observe more subtle phase changes, such as glass transitions.

2.5.5. Izod Impact testing (ASTM D 256)

2.5.5.1. Notching Specimens

In order to do notched izod test, a precise notch be cut into the specimens. The purpose of the notch is to serve as a stress concentrator. The notch is probably the most critical part of specimen preparation and there is a tight tolerances defined by ASTM D 256 on the depth of the notch (actually the material remaining under the radius of the notch), the angle of cut and the radius at the base (or apex) of the notch. Research has shown that the notch in the specimen is perhaps the greatest source of variability of test data. Since materials behave differently in response to the notching process, it is important to verify the dimensions of the notch in the specimen as opposed to verifying the cutter dimensions.

Specimens can be notched using a milling machine, engine lathe or commercially available, specifically designed notching machine. ASTM D 256 does not define the specific operation of the notching machine, but most involve adjusting the cutter height on the machine so that it cuts a notch that leaves 10.16 +/- 0.05 mm (0.400 +/- 0.002 in.) of material remaining under the apex of the notch in a single pass and a radius of curvature at the apex of 0.25 +/- 0.05 mm (0.010 +/- 0.002 in.). Single tooth cutters are preferable over multi-tooth cutters. The profile of the cutter can vary but it must produce the notch as specified in the standard.

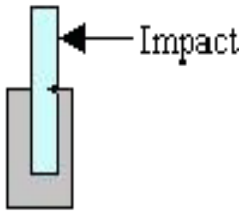

2.4.5.2. Notched Izod Impact Strength

Specimen is held as a vertical cantilevered beam and is broken by a pendulum. Impact occurs on the notched side of the specimen. Energy per unit thickness required to break a test specimen under flexural impact. Test specimen is held as a vertical cantilevered beam and is impacted by a

swinging pendulum. The energy lost by the pendulum is equated with the energy absorbed by the test specimen.

The objective of the experiment is to test the ability of different types of specimens to withstand impacts using the notched Izod impact test as specified by ASTM D256 Standard Test Method for Determining the Izod Pendulum Impact Resistance of Plastics. The Izod test method A is chosen as our test.

Figure 2.6 Impact testing machine

2.5.5.3. Laboratory Procedure

This test fixes one end of a notched specimen in a cantilever position by means of a vice. A striker on the arm of a pendulum or similar energy carrier then strikes the specimen. The dimensions of the specimen are 10mm in width, 12.7mm in depth and 63.5mm in length. A groove is prepared in the middle of the specimen, of 1.5mm depth. The energy absorbed by the specimen in the breaking process is known as the breaking energy. The breaking energy is

converted into an indication of a materials impact resistance using such units as foot-pounds or joules.

2.6 Preparation of self-healing composites

Epoxy composites containing varying amounts of USP encapsulated urea-formaldehyde (UF) microcapsules (10-30% w/w) were prepared by room temperature curing of epoxy with TETA hardener. Requisite amount of microcapsules along with 1% (w/w microcapsule) initiator AIBN was then dispersed in the epoxy resin using ultrasonication. Required amount of TETA hardener was then added to the mixture. After degassing the suspension under vacuum, it was transferred to greased silicone moulds and allowed to cure at 30°C for 24 h. For comparison purpose neat epoxy specimens were also prepared and these are designated as EP. Composite specimens containing microcapsules are designated as EP followed by the concentration of microcapsule dispersed. For example, EP10 refers to the composite specimens containing 10% microcapsules. The details of all the compositions prepared and their sample designations are presented in Table 1.

Table 1: Sample designation and compositional details

Sample Designation	Amount (g)		
	Epoxy resin	Hardener	Microcapsule
EP	100	13	-
EP10x	100	13	11.3
EP15x	100	13	16.9
EP20x	100	13	22.6
EP25x	100	13	28.2

Where x is ‘USP’ for unsaturated polyester containing microcapsules and ‘E’ for epoxy containing microcapsules

CHAPTER 3: RESULTS AND DISCUSSION

3.1 Microencapsulation of USP in polystyrene shell

3.1.1. Morphological investigations

USP encapsulated poly(styrene) microcapsules were prepared by solvent evaporation technique. The schematic of the process is presented in Figure 3.1. It can be seen that this method is relatively much simpler as compared to the conventional method of encapsulation using emulsion polymerization. Previously Li et al. have employed this method for preparation of PMMA microcapsules encapsulating polyetheramine.

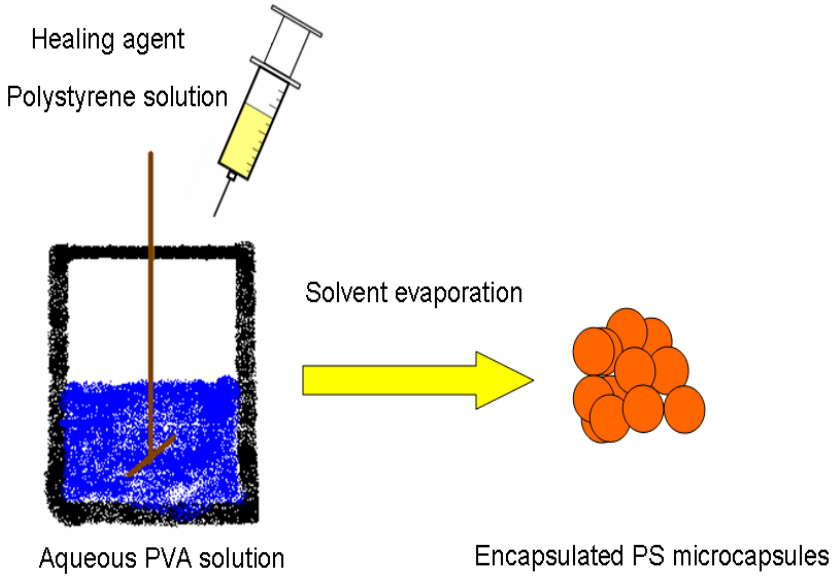

Figure 3.1: Schematic of preparation of healing agent encapsulated polystyrene microcapsules.

The SEM image of a representative batch of unsaturated polyester encapsulated polystyrene microcapsules is presented in Figure 3.2. It can be seen that the microcapsules are spherical in shape, and their surface texture was rather smooth.

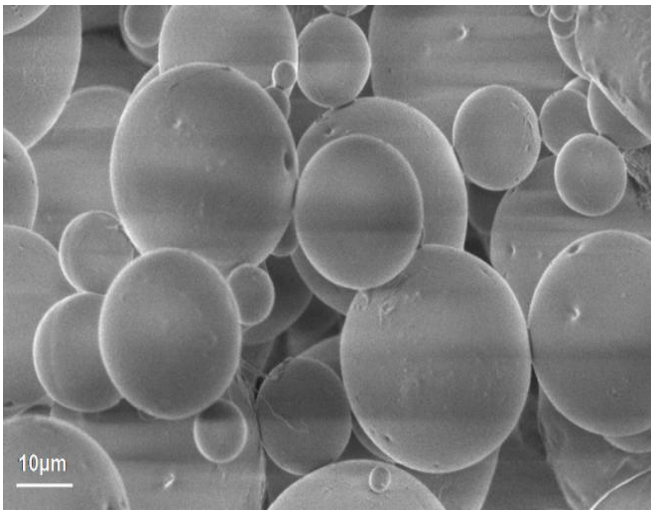

Figure 3.2: SEM image of USP encapsulated poly(styrene) microcapsules

The effect of processing conditions on the physico-chemical properties of microcapsules was established. The yield of the microcapsules, as determined by gravimetric analysis, was found to be 67 ± 5%.

3.1.2. Structural properties

The FTIR spectra of the polyester resin both before and after curing, and microcapsules are presented in Figure 3.3. The strong absorption band at 755 cm^{-1} can be attributed to -C-H bending arising from 1 and 3 positions in benzene ring. A broad absorption band at 1145 cm^{-1} confirms the presence of –C-O-C- of ester linkage. The strong absorption appearing at 1306 cm^{-1} can be assigned to –C=C– group of the polyester and the medium absorption band at 1461 cm^{-1} can be attributed to –C-H bending. The presence of –C=O and symmetric –CH stretching was confirmed by the presence of strong bend at 1736 and 2985 cm^{-1} respectively. The band at 1736 cm^{-1} further confirms the presence of –C=O ester group. An IR spectrum of the cured polyester resin is also shown in the figure. The band at around 2985 cm^{-1} becomes sharper and bands due to –CH=CH- group almost disappears. A sharp band at 1447 cm^{-1} appears in the IR spectrum of composite, which indicates the presence of alkane group, clearly attributable to the conversion of –CH=CH- group to alkane during the cross linking process. The absence of these characteristic bands in the spectra of microcapsules is clearly indicative of the complete encapsulation of the

liquid resin in poly(styrene) shell. The microcapsules exhibit absorption at 3026 and 2922 cm^{-1}, which could be attributed to the $\nu CH_{(ar)}$ and $\nu CH_{(al)}$ respectively.

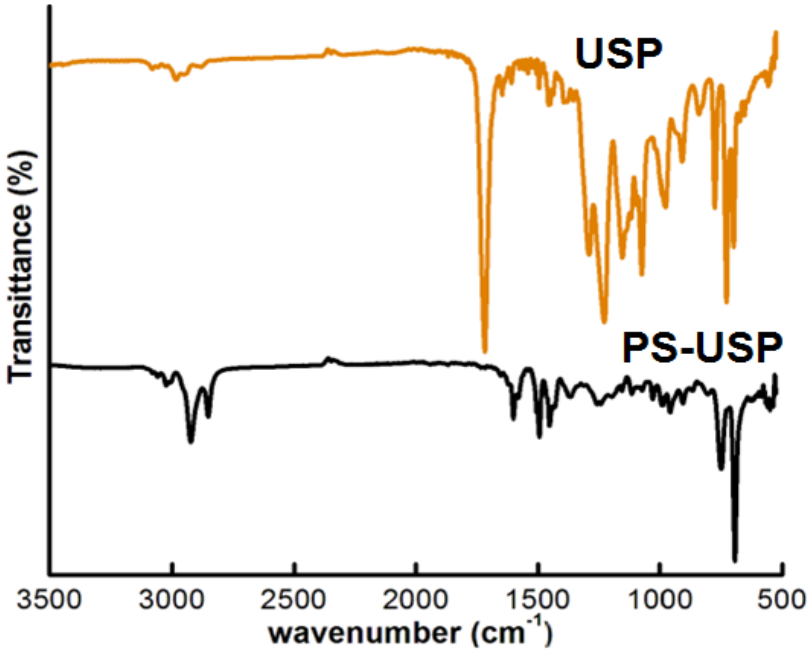

Figure 3.3: FTIR of Microcapsules, unsaturated polyester liquid

3.1.3. Thermal properties

Figure 3.4 shows the TGA traces of USP encapsulated polystyrene microcapsules and liquid polystyrene. TGA traces of liquid USP shows three step degradation behavior. The first mass loss at T< 200°C can be attributed to the loss of volatile styrene present in the polyester composition. Dynamic heating leads to the polymerization of the polyester and styrene chains and the second mass loss at 300-400°C can be attributed to the degradation of the polystyrene chain.[23] The final mass loss 400-550°C is due to decomposition of cross-linked structure of USP. The TGA trace of microcapsules exhibit a two-step degradation. First mass loss (300-400°C) is due to degradation of shell material i.e. polystyrene and subsequent mass loss (400-550°C) occurs due to the decomposition of core material i.e. USP

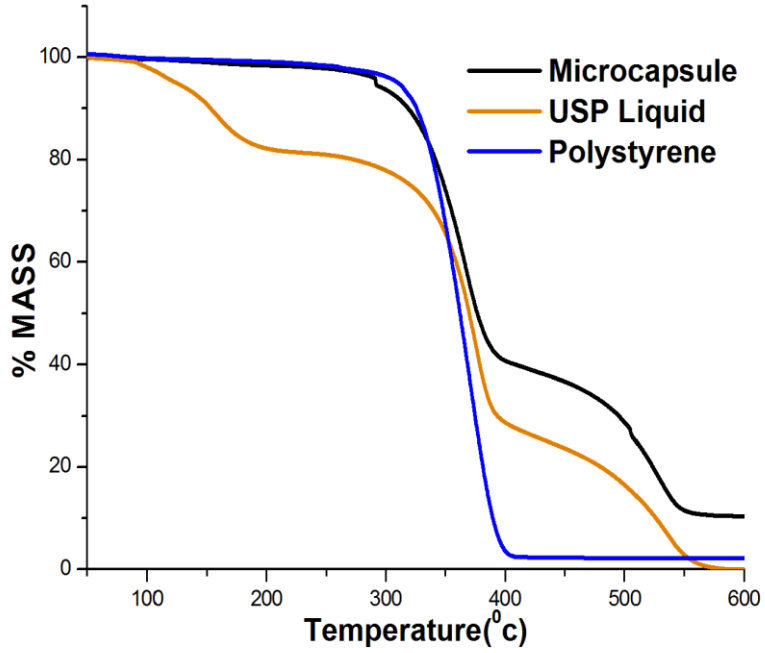

Figure 3.4: TGA of microcapsules, unsaturated polyester (USP) liquid

On the other hand, polystyrene exhibits single step degradation at 300-400°C. The major degradation product of polystyrene consists of a mixture of saturated and unsaturated compounds. It has been reported that the degradation products of polystyrene include 40% monomer, with decreasing amounts of dimer, trimer, tetramer and pentamer. The PS degradation is reportedly initiated at weak links inherent to the polymer, particularly peroxy and hydroperoxy structures. Once the weak links are consumed the major mass loss occurs due to random chain scission. Earlier studies have revealed that the TGA traces shift to higher temperature, when the degradation is performed under inert atmospheres.

3.1.4. Effect of concentration of encapsulating polymer

Core-content is one of the most important characteristics of microcapsules. In view of the similar solubilities of unsaturated polyester and PS, conventional technique of core-content quantification proved unsuccessful and the ratio of heat of curing (DSC technique) of encapsulated unsaturated polyester to that of the neat polyester was used to determine the same.

The core content was found to increase from 20% to 40 % by decreasing the PS content in the feed solution from 10% to 2% w/v, at a constant stirring speed of 500 rpm. However, the core content could not be increased further, due to the fragile nature of the shell, which appears to be incapable of cementing higher amounts of healing agent. The TGA traces of microcapsules with different core content are presented in Figure 3.5

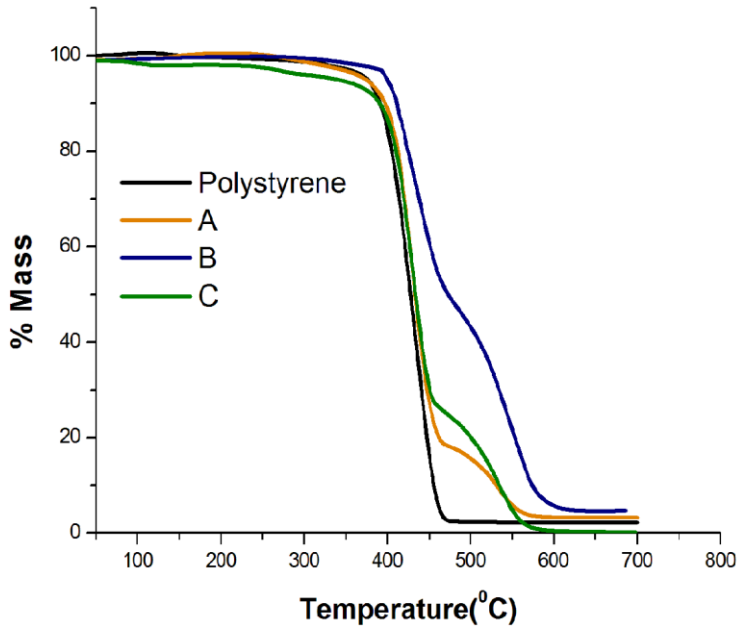

Figure 3.5: TGA of microcapsules showing the effect of concentration of encapsulating polymer. Ps: polystyrene, A: 10%, B: 6%, C: 2% w/v polystyrene

3.1.5. Effect of stirring speed

The effect of increasing stirring speed on the microcapsule dimensions is presented in Figure 3.6. As expected, increasing the rate of stirring led to a decrease in the particle dimensions, which could be attributed to the shearing of the large oily droplets into smaller microspheres under higher shear rates[24].

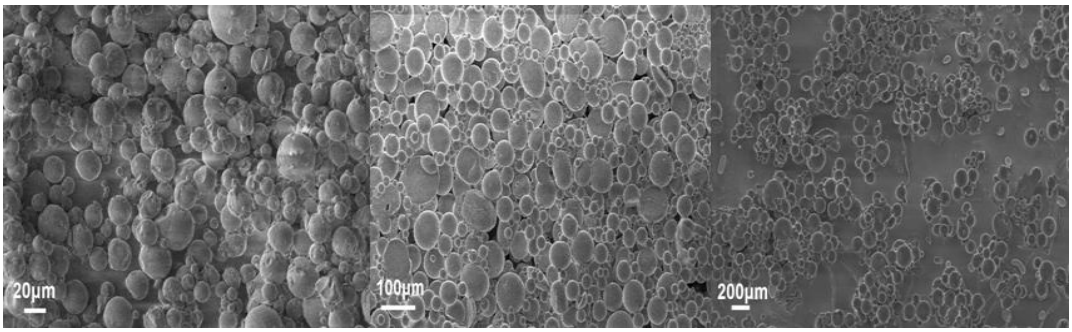

Figure 3.6: SEM image of microcapsules prepared under different stirring speeds a) 400, b) 500, c) 600 rpm. Inset shows the enlarged image of a single microcapsule.

3.2 Characterization of epoxy encapsulated polystyrene microcapsules

PS microcapsules containing cycloaliphatic epoxy resin were prepared in a similar manner as described above. The SEM image of a representative batch of epoxy encapsulated polystyrene microcapsules is presented in Figure 3.7. The microcapsules were found to possess perfectly spherical shape, with a smooth surface texture.

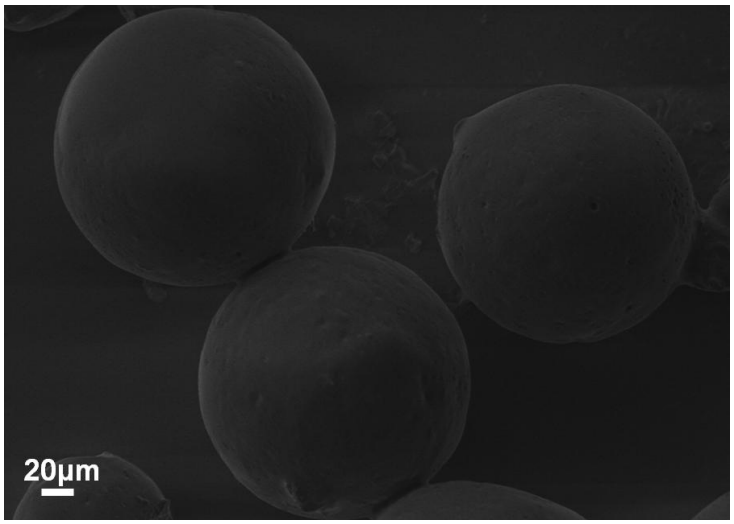

Figure 3.7: SEM image of epoxy encapsulated poly(styrene) microcapsules

The effect of processing conditions on the physico-chemical properties of microcapsules was established. The yield of the microcapsules, as determined by gravimetric analysis, was found to be 65 ± 5%.

3.2.1. Structural properties

FTIR spectra of urea formaldehyde microcapsules are presented in Figure 3.8. Other characteristic absorptions include alkyl C–H stretching (2950 cm^{-1}), C–H bending (1490 cm^{-1} and 1360 cm^{-1}), aliphatic C–N (1200 and 1170 cm^{-1}), triazine ring (1555 cm^{-1}) and C–O–C stretching (1027 cm^{-1}). The UF microcapsules also exhibited absorption in the same region, besides additional absorption at 1649 cm^{-1} due to NH-CO-NH stretching[25] .

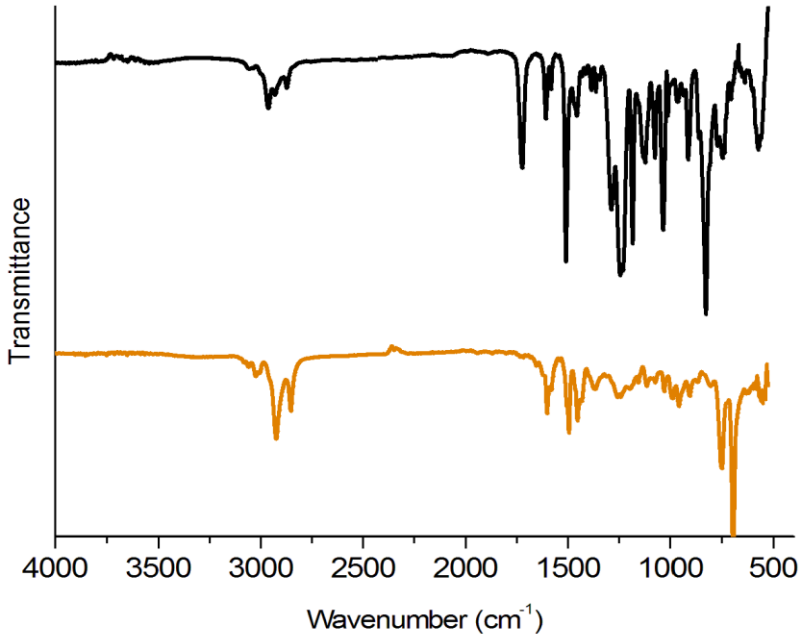

Figure 3.8 FTIR of Microcapsules, Epoxy liquid

3.2.2. Effect of stirring speed

The effect of increasing stirring speed on the microcapsule dimensions is presented in Figure 3.9. As expected, increasing the rate of stirring led to a decrease in the particle dimensions, which could be attributed to the shearing of the large oily droplets into smaller microspheres under higher shear rates[24].

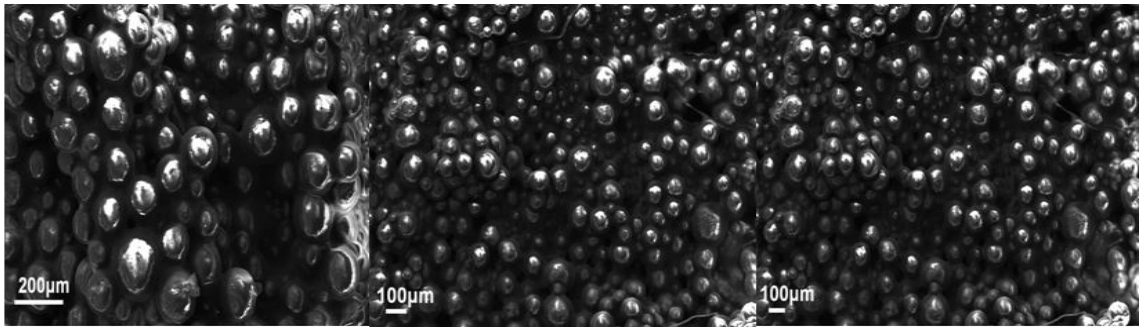

Figure 3.9: SEM image of microcapsules prepared under different stirring speeds a) 400, b) 500, c) 600 rpm. Inset shows the enlarged image of a single microcapsule.

3.3 Characterization of epoxy encapsulated urea-formaldehyde microcapsules

Healing agent encapsulated microcapsules were prepared by emulsion polymerization route. The core content of the microcapsules as determined by gravimetric analysis was found to be 56 ± 2 %. SEM image of a representative batch of epoxy encapsulated urea-formaldehyde microcapsules is presented in Figure 3.10.

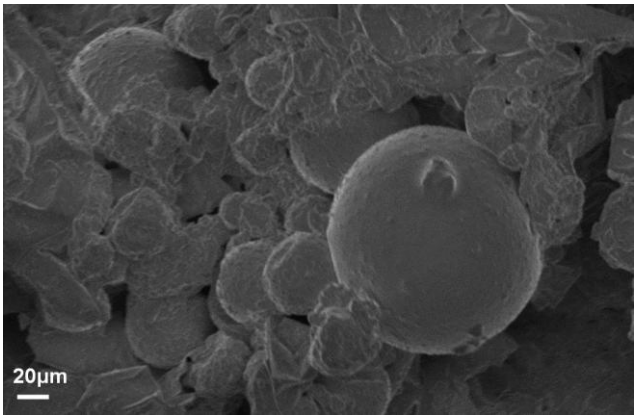

Figure 3.10: SEM image of USP microcapsules

3.3.1. Thermal properties of microcapsules

The TG traces of epoxy encapsulated UF microcapsules are presented in Figure 3.11. It can be seen the UF microcapsules exhibit first mass loss occurs due to the transformation of methylene ether bridges into methylene bridges at ~200°C, a phenomenon associated with loss of

formaldehyde. The subsequent mass loss at 300°C-390°C occurs due to pyrolytic degradation of the cross-linked network.

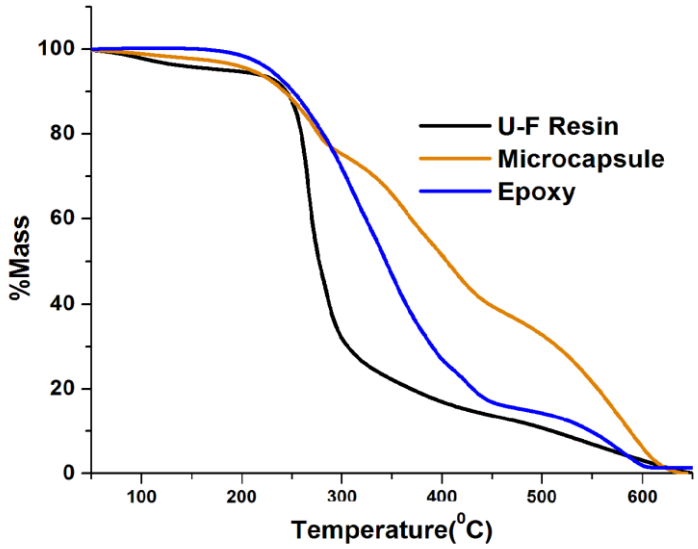

Figure 3.11: TGA of microcapsules, epoxy liquid

3.2.2. Structural properties

FTIR spectra of urea formaldehyde microcapsules are presented in Figure 3.12. Microcapsules shows characteristic bands at 3350 cm^{-1}(overlapping absorptions of hydroxyl, imino and amino functionalities),2962 cm^{-1}(alkyl C–H stretching),1255 and 1181 cm^{-1}(aliphatic C–N), 1649 cm^{-1} (NH-CO-NH stretching) and 1034 cm^{-1}(C–O–C stretching).[25] The spectra of microcapsule are matching with that of the UF resin and different from the spectra of liquid unsaturated polyester. A medium absorption band at 1456 cm^{-1} can be attributed to –C-H bending. The presence of –C=O and symmetric –CH stretching was confirmed by the presence of strong bend at 1717 cm^{-1} and 2983 cm^{-1} respectively.[19] Other characteristic absorptions include alkyl C–H stretching (2950 cm^{-1}), C–H bending (1490 cm^{-1} and 1360 cm^{-1}), aliphatic C–N (1200 and 1170 cm^{-1}), triazine ring (1555 cm^{-1}) and C–O–C stretching (1027 cm^{-1}). The UF microcapsules also

exhibited absorption in the same region, besides additional absorption at 1649 cm^{-1} due to NH-CO-NH stretching[25].

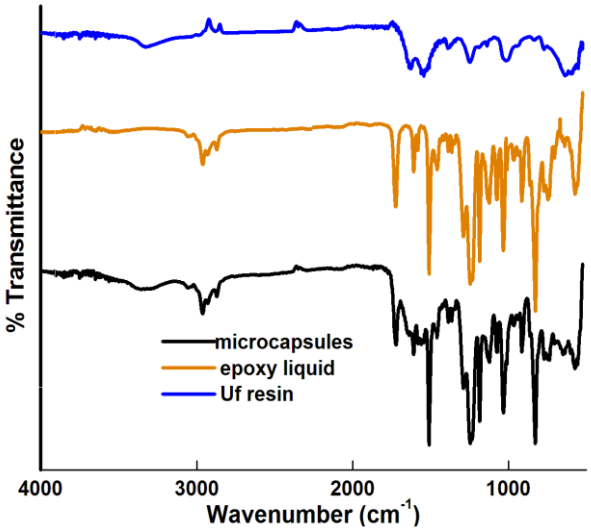

Figure 3.12: FTIR of UF resin, microcapsule, and epoxy

3.2.3. Latent curing system

2-methyl imidazole was reacted with copper chloride to prepare a complex, the proposed structure of which is presented in Figure 3.13.

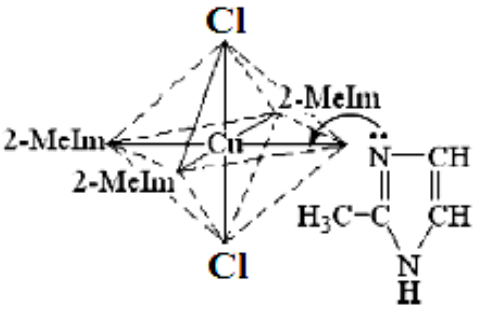

Figure 3.13: Structure of 2-methyl imidazole

The TGA traces of 2-methyl imidazole and the copper complex are presented in Figure 3.14. It can be seen that 2-methylimidazole decomposes at low temperature (T onset = 150°C) while the copper complex is relatively more thermally stable. It has been reported that the complex possesses long-term stability, and is dissociated into $CuCl_2$ and 2-methylimidazole again at around 130–170°C.

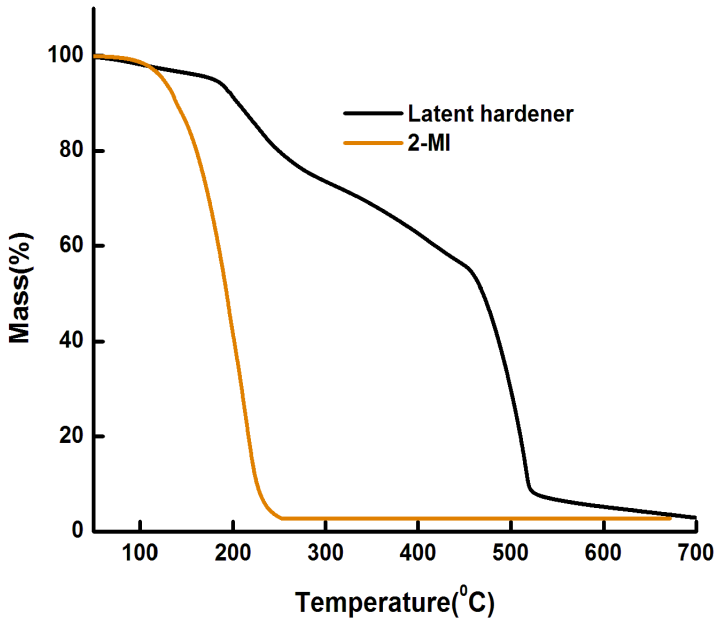

Figure 3.14: Thermogravimetric traces of 2methyl imidazole and its copper complex.

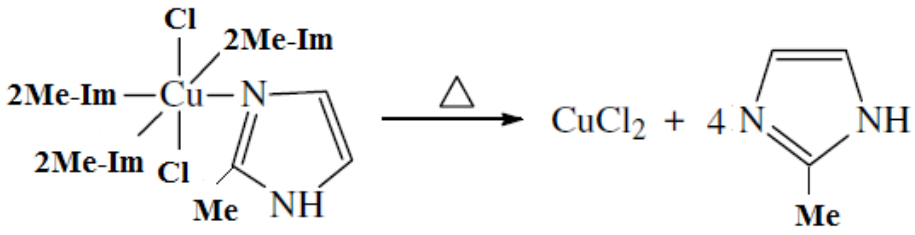

Scheme 3- Decomposition of latent hardener to release 2-methyl imidazole.

Taking advantage of this habit, curing of the released epoxy healing agent catalyzed by 2-methylimidazole (i.e. cracks healing) can be triggered at the dissociation temperature of $CuCl_2$ $(2\text{-MeIm})_4$, which is higher than the curing temperature of epoxy.

The curing reaction of epoxy with the latent hardener was studied using DSC under non-isothermal conditions. The DSC trace is presented in Figure 3.15. It can be seen that the curing reaction initiates at temperature 150°C.

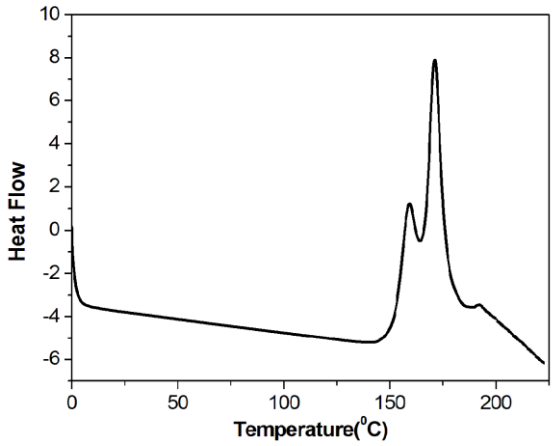

Figure 3.15: Non-isothermal DSC scans of $CuBr_2(2\text{-MeIm})_4$–epoxy system(1 wt%)

3.2.4. Structural properties

The Figure 3.16 shows all the characteristic bands for imidazole including N-H stretching (3300 cm^{-1}), N-H wagging vibration (756 cm^{-1}), C-N stretching (1110 cm^{-1}), C=N stretching (1600 cm^{-1}), C=C stretching (1680 cm-1) and =CH rocking vibration (1440 cm^{-1}) [26]. Therefore, it is clear that the imidazole in $CuCl_2(2\text{-MeIm})_4$ retains the original structure. However, the most significant difference in the two spectra is that the C-H stretching absorptions in methyl side group and imidazole ring at 2500–3200 cm^{-1} disappear in the spectrum of complex. It can be attributed to the fact that the coordination might have obstructed certain vibration modes.

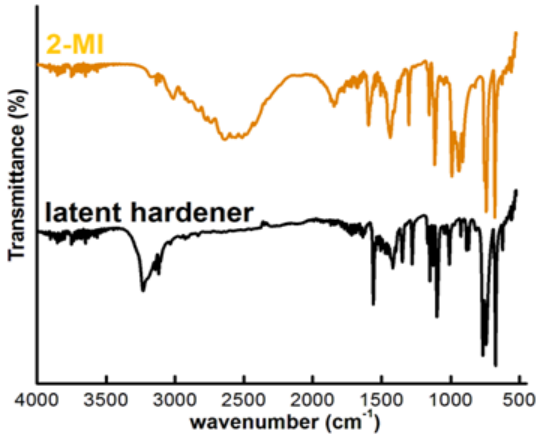

Figure 3.16: FTIR of 2-imidazole, copper-imidazole complex (LCA)

3.2.5. Impact strength of self-healing composites containing latent hardener.

Introduction of microcapsules led to a decrease in the impact strength of the samples as is evident from the following figure. (Figure 3.17)

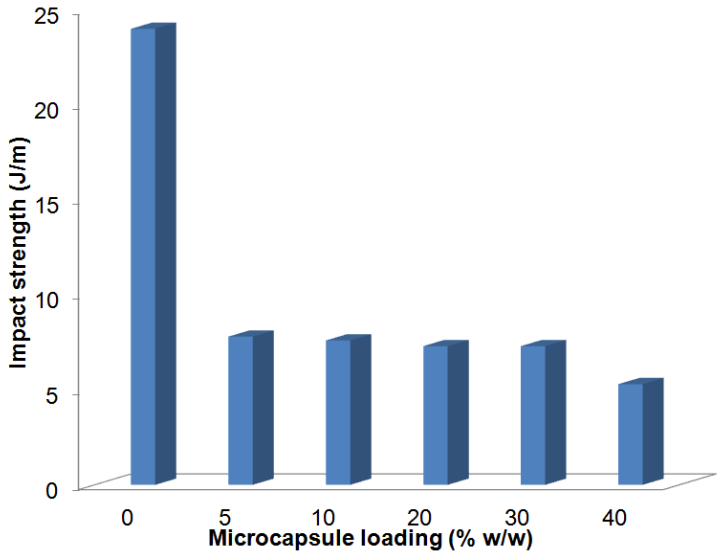

Figure 3.17: Impact strength of microcapsules

This behavior is not unexpected in view of the fragile nature of the microcapsules. It has been reported previously that the presence of microcapsules lead to substantial decrease in quasi-static mechanical properties like tensile strength, modulus and elongation. It is to be noted however that their introduction leads to appreciable increase in the fracture toughness.

3.2.6. Self-Healing Efficiency

For quantification of self-healing efficiency, the impact tested samples were joined and allowed to heal at elevated temperatures. Self-Healing efficiency was calculated as a ratio of healed to virgin impact strength [21]. For comparison purposes, a set of samples was prepared in the absence of LCA. It was interesting to note that samples containing epoxy loaded microcapsules healed even in the absence of LCA, however the temperature required for healing was rather high (150ºC). To decrease the healing temperature, LCA (1% w/w microcapsule) were included in the liquid resin prior to curing. This led to substantial decrease in the healing temperature, which

could be brought down to 150ºC. The effect of increasing microcapsule loading on the self-healing efficiency was also investigated. The increase in self-healing efficiency as a function of microcapsule loading is presented in Figure 3.18. It can be seen that the healing efficiency increases with microcapsule loading and the maximum value (62 ±5 %) is obtained for the 30 % (w/w) of epoxy encapsulated microcapsule.

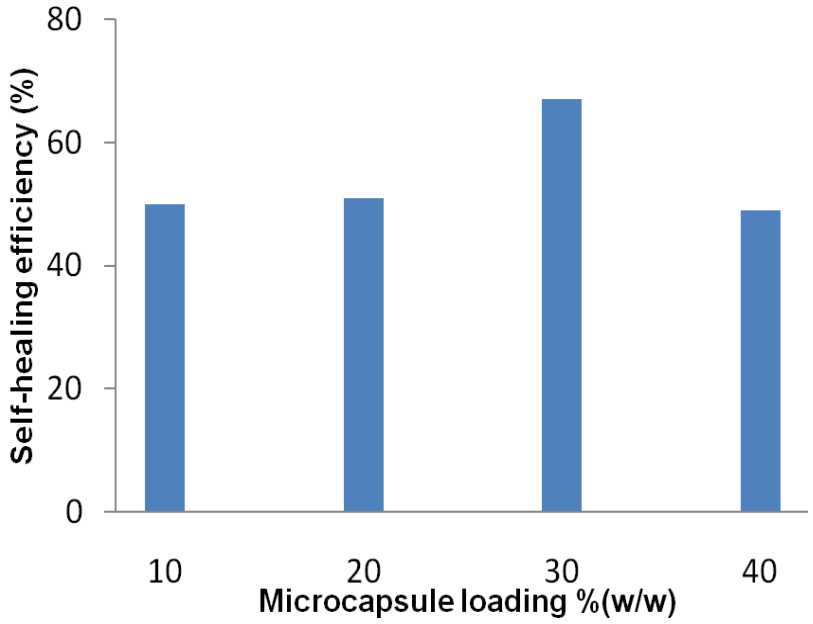

Figure 3.18: Self-healing efficiencies of self-healing composites

3.3 Characterization of USP encapsulated UF microcapsules

USP encapsulated microcapsules were prepared by emulsion polymerization route. The core content of the microcapsules as determined by gravimetric analysis was found to be 58 ± 4 %. The SEM image of a representative batch of unsaturated polyester encapsulated urea-formaldehyde microcapsules is presented in Figure 3.19.

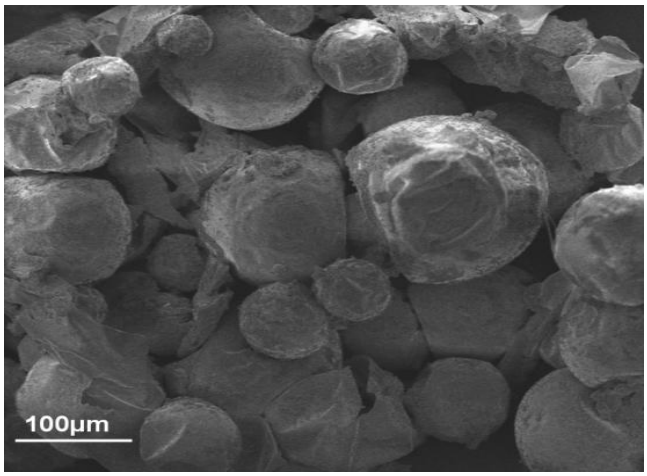

Figure 3.19: SEM image of USP microcapsules

It can be seen that the microcapsules are spherical in shape, and their surface texture is rough, which could be attributed to the presence of urea-formaldehyde resin nanoparticles on the surface[12]. The formation of urea-formaldehyde is a two-step process. The reaction of urea with formaldehyde results in the formation of monomethylol and dimethylol urea which subsequently undergo condensation reaction to form a linear polyurea-formaldehyde polymer as shown in Scheme 4.

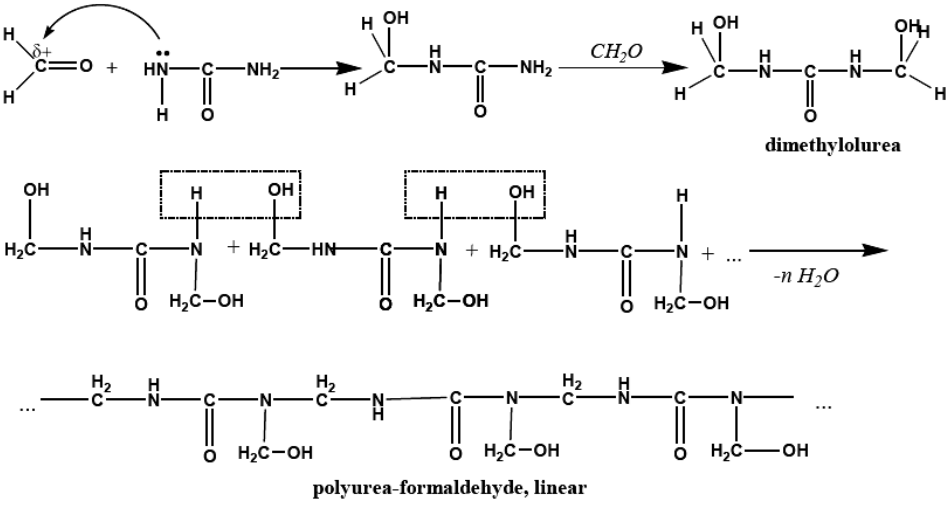

Scheme 4- Polymerisation reaction of Urea and Formaldehyde

3.3.1. Microcapsule dimensions

The microcapsule size could be controlled by varying the rate of agitation during the polymerization process. In general, with increasing stirring rate, the microcapsule dimensions decrease, which can be attributed to the shearing of the oily droplets at higher agitation. However, for the present study, a stirring speed of 350 rpm was employed, which yielded microcapsules of desired dimensions for their use in self-healing application,[12] i.e. (diameter ~130 ± 49 μm).

3.3.2. Core content

Core content is one of the most important parameter of healing agent loaded carriers. The core content was determined gravimetrically as the ratio of encapsulated mass of healing agent to the initial mass of the microcapsules. In the present study, the core content of the microcapsules was 58± 4 %.

3.3.3. Structural properties

FTIR spectra of urea formaldehyde microcapsules are presented in Figure 3.20. Microcapsules shows characteristic bands at 3350 cm^{-1}(overlapping absorptions of hydroxyl, imino and amino functionalities),2962 cm^{-1}(alkyl C–H stretching),1255 and 1181 cm^{-1}(aliphatic C–N), 1649 cm^{-1} (NH-CO-NH stretching) and 1034 cm^{-1}(C–O–C stretching).[25] The spectra of microcapsule are matching with that of the UF resin and different from the spectra of liquid unsaturated polyester. Spectra of USP exhibit a strong absorption band at 777 cm^{-1} and a weak band at 1073 cm^{-1} due to -C-H bending arising from 1 and 3 positions in benzene ring. A broad-spectrum absorption band at 1153 cm^{-1} is for the presence of –C-O-C- of ester linkage. A strong absorption peak appearing at 1289 cm^{-1} was assigned to –C=C– group of polyester. A medium absorption band at 1456 cm^{-1} can be attributed to –C-H bending. The presence of –C=O and symmetric –CH stretching was confirmed by the presence of strong bend at 1717 cm^{-1} and 2983 cm^{-1} respectively.[19]

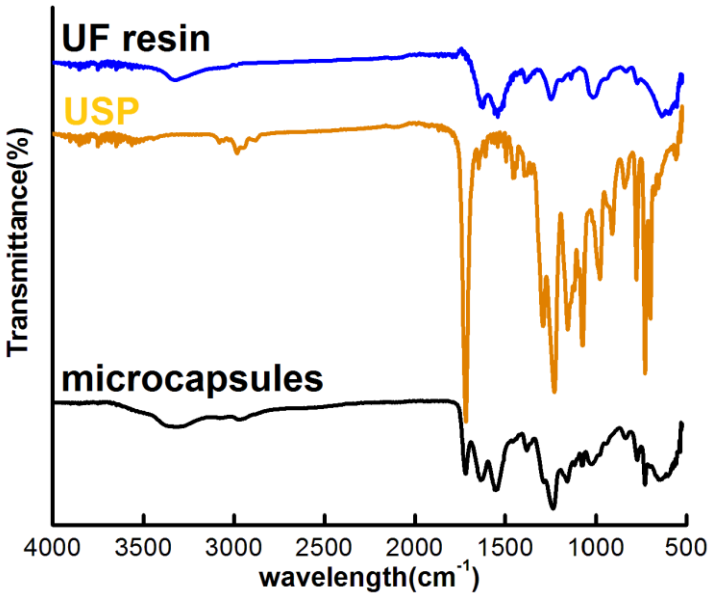

Figure 3.20: FTIR of Microcapsules, unsaturated polyester liquid and urea-formaldehyde resin

3.3.4. Thermal properties of microcapsules

The TG traces of unsaturated polyester encapsulated UF microcapsules are presented in Figure 3.21. For comparison purposes, the thermal degradation behavior of the neat USP and urea-formaldehyde resin is also presented. These TGA traces give supporting evidence for the FTIR analysis. As illustrated in Figure 3, for the urea-formaldehyde resin the initial loss ~T < 150℃ may be due to removal of water followed by the onset of pyrolysis of urea–formaldehyde resin at about 242℃ (maximum rate of pyrolysis being ~ 270℃) and > 400℃ .Unsaturated polyester (USP) liquid shows initial mass loss< 150℃ due to evaporation of styrene present in the resin. The subsequent mass loss at ~ 350 and 450℃ may be attributed to the cross linking and pyrolysis of cross-linked structure. It is interesting to note that the curve of the USP encapsulated microcapsule consist of two stages of weight loss. Accordingly, the temperatures of the maximum rates of pyrolysis are about 350-370°C and ~450°C, respectively. They should result from the thermal degradation of the shell (urea–formaldehyde resin) and the core (unsaturated polyester) of the microcapsules. Compared to the pristine unsaturated polyester

(USP), thermal stability of the USP in the microcapsule is evidently increased owing to the protection of the shield of the urea–formaldehyde wall.

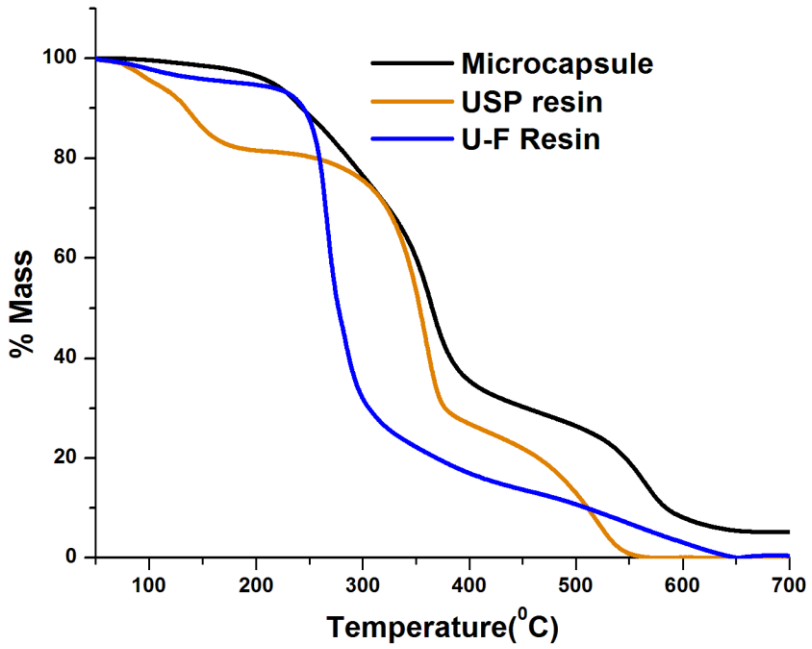

Figure 3.21: TGA of microcapsules, unsaturated polyester (USP) liquid and urea-formaldehyde (UF) resin

3.3.5. Epoxy-Microcapsule composite

Epoxy composites were prepared by dispersing requisite amounts of UF microcapsules containing unsaturated polyester in epoxy resin by ultrasonication, followed by curing with TETA hardener under ambient conditions. The TG trace of cured epoxy and its composites with different microcapsules is presented in Figure 3.22. It can be seen that the introduction of epoxy encapsulated microcapsules has no effect on the thermal stability of the base polymer.

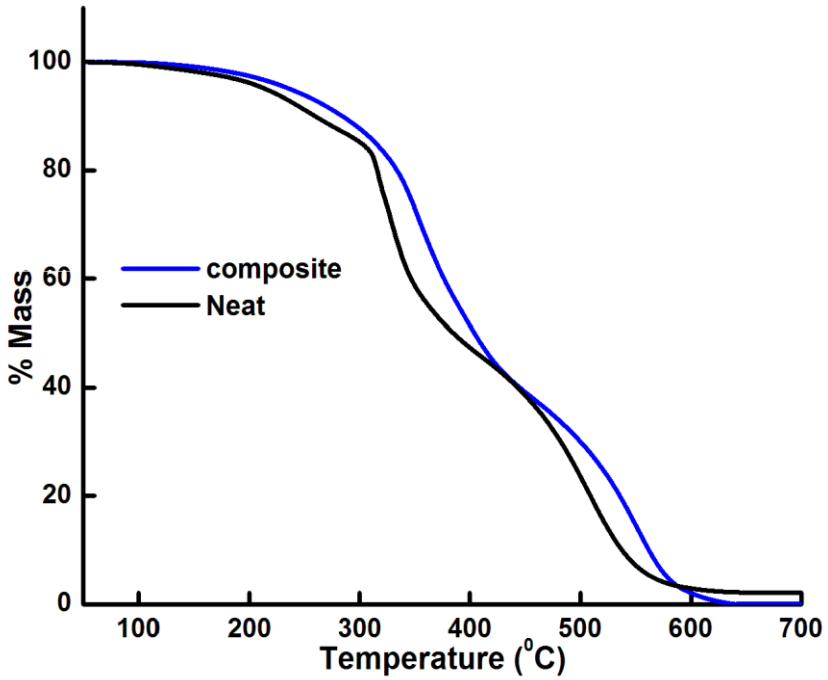

Figure 3.22: TG traces of composites formed with microcapsules

3.3.6. Impact strength of self-healing composites containing AIBN

Introduction of microcapsules led to a decrease in the impact strength of the samples as is evident from the following figure. (Figure 3.23)

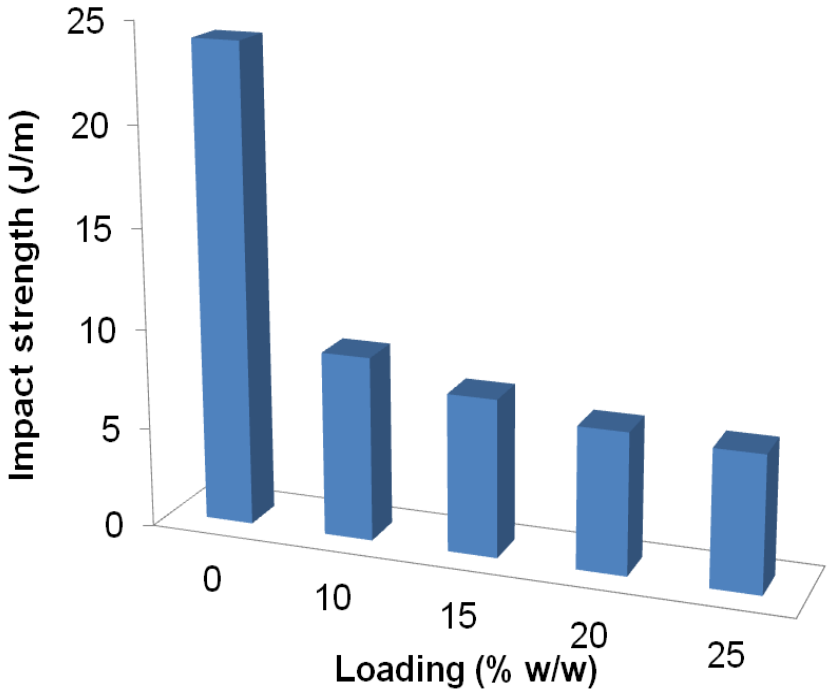

Figure 3.23: Impact strength of microcapsules

This behavior is not unexpected in view of the fragile nature of the microcapsules. It has been reported previously that the presence of microcapsules lead to substantial decrease in quasi-static mechanical properties like tensile strength, modulus and elongation. It is to be noted however that their introduction leads to appreciable increase in the fracture toughness.

3.4 Self-Healing Efficiency

For quantification of self-healing efficiency, the impact tested samples were joined and allowed to heal at elevated temperatures. Self-Healing efficiency was calculated as a ratio of healed to virgin impact strength [21]. For comparison purposes, a set of samples was prepared in the absence of AIBN. It was interesting to note that samples containing USP loaded microcapsules healed even in the absence of AIBN, however the temperature required for healing was rather high (150ºC). To decrease the healing temperature, AIBN crystals (1% w/w microcapsule) were included in the liquid resin prior to curing. This led to substantial decrease in the healing temperature, which could be brought down to 110ºC.

The curing of unsaturated polyester resin using AIBN was studied using non-isothermal DSC studies. The DSC trace is presented in Figure 3.24.

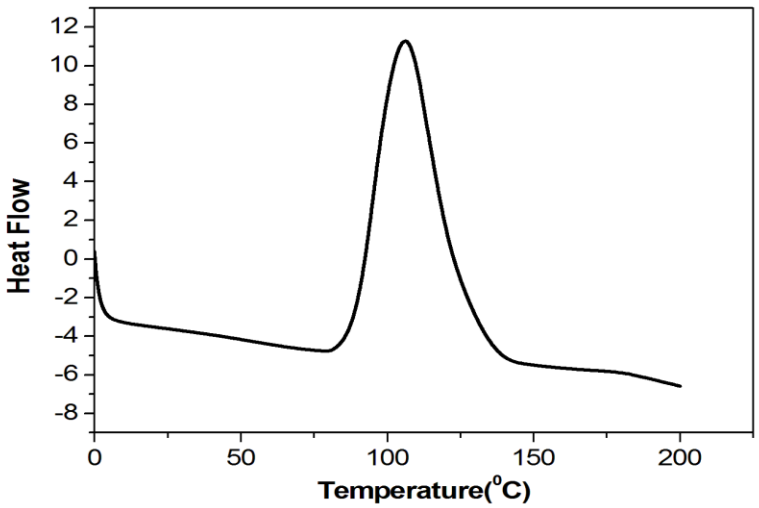

Figure 3.24: Non-isothermal DSC scans of AIBN-USP microcapsule (1 wt %)

It can be seen that the AIBN is capable of initiating the curing reaction at temperatures as low as 80ºC. However self-healing studies revealed that a temperature of 110 ºC was required to ensure complete polymerization of the USP.

The effect of increasing microcapsule loading on the self-healing efficiency was also investigated. The increase in self-healing efficiency as a function of microcapsule loading is presented in Figure 3.25. It can be seen that the healing efficiency increases with microcapsule loading and the maximum value (103 ±5 %) is obtained for the 20 % (w/w) of USP encapsulated microcapsule.

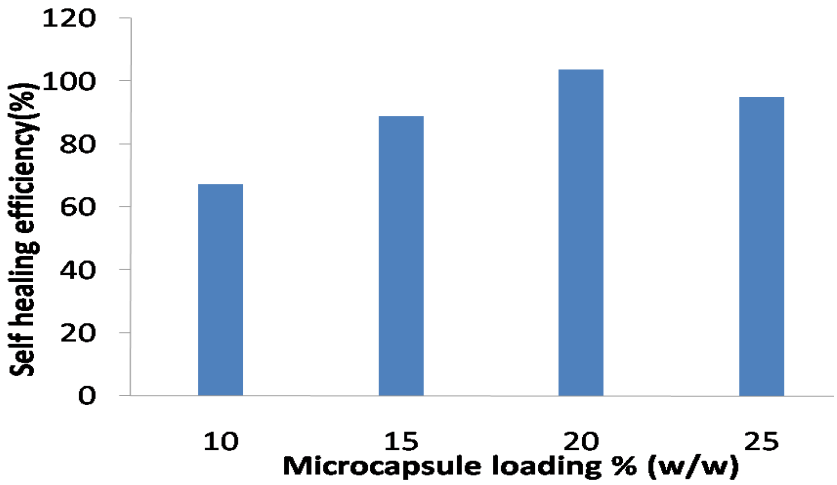

Figure 3.25: Self-healing efficiencies of self-healing composites

Fractography was performed on the cracked surfaces, and the results are presented in Figure 3.26 and 3.27. The SEM image of neat epoxy is presented in Figure 3.26. The smooth and featureless surface of epoxy is characteristic of fracture in a brittle thermosetting polymer, which exhibits no signs of plastic deformation[27,28] .

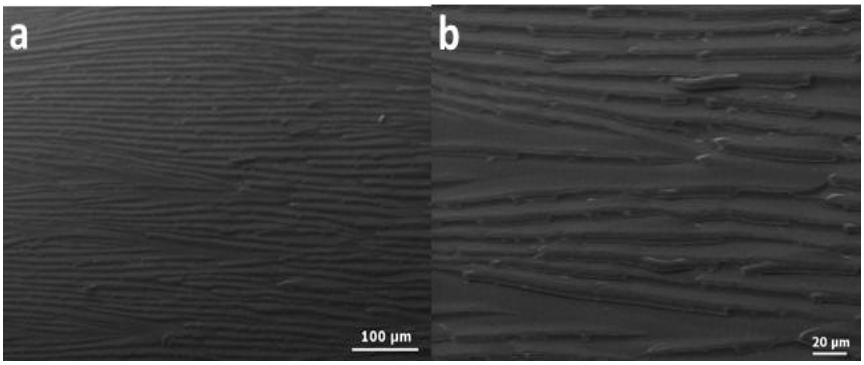

Figure 3.26: Fracture surface of neat epoxy at different magnifications.

Images were also captured along the fracture surface. The presence of feather-like hackle markings resulting from small-scale secondary crack formation could be observed just after the plastic zone which extends to the stress zone. The hackle markings transition into striations in the direction of crack propagation and finally there is a complete transition to a mirror fracture surface, as reported previously[29] .

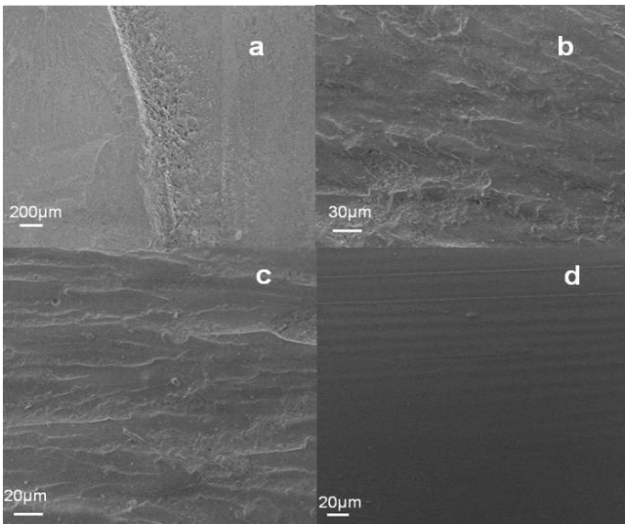

Figure 3.27: Scanning electron micrographs of fracture plane in: (a) Pre-crack tip location (b) hackle markings following plastic zone, and (c) transition zone from hackle marking to mirror fracture surface, and (d) Mirror surface of brittle fracture plane extending the length of the specimen. **Note**: The crack propagation is from left to right in all images.

In comparison, the fractured surface of the unsaturated polyester (USP) containing microcapsules was found to be rather rough throughout the crack plane. Toughening by "crack pinning" is most commonly cited to explain the toughened nature of such compositions. According to this, the role of second phase is to cause the crack front to bow out, propagation of which requires much larger amount of energy. Indirect evidence of the occurrence of this mechanism is the presence of 'tails' associated with the embedded microcapsules (Figure 3.28). In certain cases, the crack front is forced to change its path as it approaches the microcapsules, a phenomenon more commonly known as crack bowing, (Figure 3.29), which results in increased surface area. Further, the mode I character of the crack opening is also reduced, which in turn requires larger amount of energy for its propagation.

As expected, a number of "broken" microcapsules were observed on the surface of the composite. It appears that the "breaking" of the microcapsule leads to the flow of the encapsulated healant into the crack plane. In rigid particle-epoxy composites [30], crack pinning by the filler material is expected to contribute significantly towards increasing the toughness of the composite. However, in the present scenario, due to the fragile nature of the microcapsules, the contribution of this route is practically negligible.

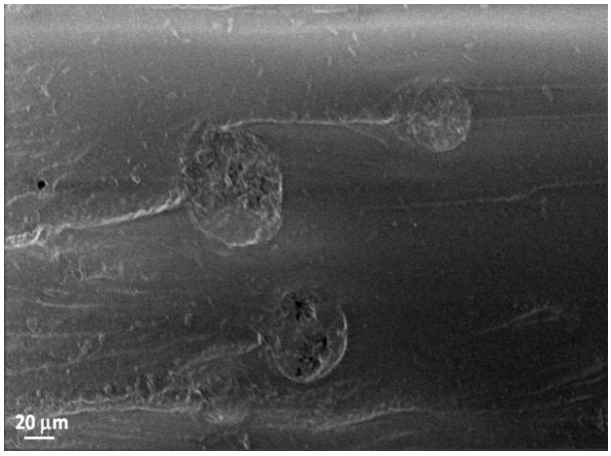

Figure 3.28: Scanning electron micrographs of fracture surface of healed sample

SEM image of the healed specimen (fracture surface) is presented in (Figure 3.29). Solidified USP can be seen in the vicinity of the microcapsules. The same has been highlighted for easy visualisation.

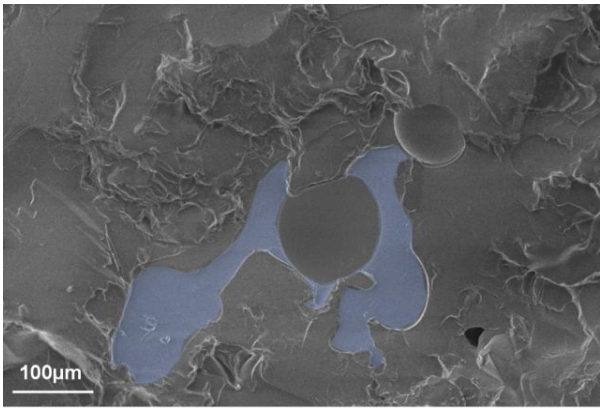

Figure 3.29: Scanning electron micrographs of fracture surface of healed sample

CHAPTER 4: SUMMARY AND CONCLUSION

4.1 Conclusion

- Different healing agents, namely unsaturated polyester and epoxy were encapsulated in polystyrene by physical encapsulation technique. Microcapsules with dimensions 140-190 microns could be obtained by this route.

- The effect of operating parameters on the microcapsule dimensions and morphology was established by SEM imaging.

- Core content of PS microcapsules, irrespective of the healing agent within was found to be 45 ± 3 %.

- Epoxy and USP were encapsulated in urea-formaldehyde microcapsules by emulsion polymerization route.

- The core content of the microcapsules was determined by solvent extraction method and was found to be 58± 4 %.

- Latent hardener (copper complex of 2 methyl imidazole) was synthesized by the reaction of copper chloride with 2 methyl imidazole. Curing reaction of epoxy with the latent hardener was studied using differential scanning Calorimetry

- Self-healing composites were prepared by dispersing varying amount of microcapsules (10-30% w/w) in the matrix.

- The impact strength was found to decrease with introduction of microcapsules in the composition.

- Latent hardener was used as a curing agent to effect self healing in epoxy compositions containing UF encapsulated epoxy microcapsules.

- Self healing efficiency was determined as the ratio of impact strength of the samples before and after healing. ~67% efficiency could be achieved using copper complex as the latent hardener system.

- Self healing was also attempted in compositions containing UF encapsulated unsaturated polyester microcapsules.

- The temperature required for curing could be brought down significantly by using AIBN as the free radical initiator. Self healing efficiency of 103% could be achieved using AIBN as the curing agent.

REFERENCES

1. Blaiszik, B. J., Polymer 50 990 2009.
2. Dry, C., Composite Structures 35, 263 1996.
3. Bleay, S. M.; Loader, C. B.; Hawyes, V. J.; Humberstone, L.; Curtis, P. T., Composites Part A: Applied Science and Manufacturing 32, 1767 2001.
4. Toohey, K. S.; Sottos, N. R.; Lewis, J. A.; Moore, J. S.; White, S. R., Nat Mater 6, 581 2007.
5. Song, Y.-K.; Chung, C.-M., Polymer Chemistry 4, 4940 2013.
6. Y. C. Yuan, eXPRESS Polymer Letters 2,, 238 2008, .
7. B. Stavrinidis, D. G. H., Physics and Chemistry of Glasses 24, 19 1983.
8. H. C. Hsieh, T. J. Y., S. Lee, Polymer 42, 1227 2001.
9. X. X. Chen, F. W., A. K. Mal, H. B. Shen, S. R. Nutt, Macromolecules 36, 1802 2003.
10. Sriram, S. R., Univeristy of Illinois at Urbana-Champaign,2001.
11. White, S. R.; Sottos, N. R.; Geubelle, P. H.; Moore, J. S.; Kessler, M. R.; Sriram, S. R.; Brown, E. N.; Viswanathan, S., Nature 409, 794 2001.
12. Brown, E. N., Journal of microencapsulation 20, 719 2003.
13. Rule, J. D.; Brown, E. N.; Sottos, N. R.; White, S. R.; Moore, J. S., Advanced Materials 17, 205 2005.
14. Rule, J. D., University of Illinois at Urban-Champaign2005.
15. Yuan, L.; Liang, G.; Xie, J.; Li, L.; Guo, J., Polymer 47, 5338 2006.
16. Roy, P.; Iqbal, N.; Kumar, D.; Rajagopal, C., Journal of Polymer Research 21, 1 2014.
17. Bauer, R. S.; Stewart, S. L.; Stenzenberger, H. D. In Kirk-Othmer Encyclopedia of Chemical Technology; John Wiley & Sons, Inc., 2000.
18. Blaiszik, B. J.; Sottos, N. R.; White, S. R., Composites Science and Technology 68, 978 2008.
19. Dholakiya, B., Unsaturated Polyester Resin for Specialty Applications, 2012.
20. Brown, E. N.; Sottos, N. R.; White, S. R., Experimental Mechanics 42, 372 2002.
21. Yuan, C. e.; Zhang, M. Q.; Rong, M. Z., Journal of Materials Chemistry A 2, 6558 2014.
22. Sánchez, L.; Sánchez, P.; Lucas, A.; Carmona, M.; Rodríguez, J., Colloid Polym Sci 285, 1377 2007.
23. al., R. D. e., Polymer Degradation and Stability 81, 473 2003.
24. Chaudhary, S.; Parthasarathy, S.; Kumar, D.; Rajagopal, C.; Roy, P. K., Polymer Composites DOI: 10.1002/pc.229272014.
25. Salaün, F.; Vroman, I., European Polymer Journal 44, 849 2008.
26. Yin, T., Composites Science and Technology 67, 201 2007.
27. Williams, J. G., Composites Science and Technology 70, 885 2010.
28. Voo, R.; Mariatti, M.; Sim, L. C., Composites Part B: Engineering 43, 3037 2012.
29. Brown, E. N.; White, S. R.; Sottos, N. R., Journal of Materials Science 39, 1703 2004.
30. Roy, P. K.; Ullas, A. V.; Chaudhary, S.; Mangla, V.; Sharma, P.; Kumar, D.; Rajagopal, C., Iranian Polymer Journal 22, 709 2013.